We are IntechOpen, the world's leading publisher of Open Access books Built by scientists, for scientists

4,800
Open access books available

122,000
International authors and editors

135M
Downloads

Our authors are among the

154
Countries delivered to

TOP 1%
most cited scientists

12.2%
Contributors from top 500 universities

CLARIVATE ANALYTICS BOOK CITATION INDEX INDEXED

WEB OF SCIENCE™

Selection of our books indexed in the Book Citation Index in Web of Science™ Core Collection (BKCI)

Interested in publishing with us?
Contact book.department@intechopen.com

Numbers displayed above are based on latest data collected.
For more information visit www.intechopen.com

14

Recent Advances in the Modeling of PEG Hydrogel Membranes for Biomedical Applications

T. Ipek Ergenç and Seda Kızılel
Koc University
Department of Chemical and Biological Engineering Istanbul, Turkey

1. Introduction

PEG hydrogels have been studied intensively as tissue engineering scaffolds because they can provide a highly swollen three dimensional (3-D) environment similar to soft tissues and allow diffusion of nutrients and cellular waste through the elastic networks. (Lee and Mooney 2001; Hoffman 2002) PEG has played a significant role as hydrophilic polymer for biomedical applications which include surface modification, bioconjugation, drug delivery and tissue engineering due to the critical properties such as resistance to protein adsorption, biocompatibility, non-immunogenecity. (Lee, Lee and Andrade 1995; Alcantar, Aydil and Israelachvili 2000) PEG has a basic structure, known as PEG diol with two hydroxyl end groups which can be utilized to be converted into other functional groups for conjugation of biomolecules. (Peppas, Keys, Torres-Lugo and Lowman 1999) These functional groups consists of methyloxyl, carboxyl, amine, thiol, azide, vinyl sulfone, azide, acetylene, and acrylate. PEG also has either linear or branched (multiarm or star) structures (Scheme 1).
Several approaches have been used to synthesize crosslinked PEG hydrogels, such as free radical photopolymerization of PEG acrylates,(Elisseeff, Anseth, Sims, McIntosh, Randolph and Langer 1999; Buxton, J Zhu, Marchant, West, Yoo and Johnstone 2007; Hahn, McHale, Wang, Schmedlen and West 2007; Beamish, Zhu, Kottke-Marchant and Marchant 2010; Hubbell 1998; Kizilel, Perez-Luna and Teymour 2004; Kizilel, Sawardecker, Teymour and Perez-Luna 2006) and chemical reactions that include condensation, (Hubbell 1998) Michael type addition,(Metters and Hubbell 2005; Park, Lutolf, Hubbell, Hunziker and M 2004) click chemistry,(Polizzotti, Fairbanks and Anseth 2008; Malkoch et al. 2006) native chemical ligation,(Hu, Su and Messersmith 2009) and enzymatic reaction. (Sanborn, Messersmith and Barron 2002; Ehrbar et al. 2007; Ehrbar, Rizzi, Schoenmakers, BS, JA, Weber and Lutolf 2007) Among these approaches, the synthesis of PEG hydrogels through photopolymerization is the most common approach which uses light to convert PEG prepolymer solutions into crosslinked insoluble hydrogels. This technique not only allows the synthesis of hydrogel scaffolds with spatial and temporal control, it is also utilized for encapsulation of cells and biological molecules at physiological temperature and pH. (Truong and West 2002; Fisher, Dean, Engel and Mikos 2001) The major type of macromers used for photopolymerization includes PEG diacrylates (PEGDA), multiarm PEG acrylate

(n-PEG-acr), and PEG dimethacrylate (PEGDMA). PEG hydrogels can be modified to be degradable through incorporation of degradable segments, such as polyester, (Sawhney, Pathak and Hubbell 1993; Clapper, Skeie, Mullins and Guymon 2007; Jiang, Hao, You, Liu, Wang and Deng 2008) polypropylene fumarate (PPF),(Kretlow, Klouda and Mikos 2007; S'Engel and Mikos 2000) acetal,(Ksihara, Matsumura and Fisher 2008) and disulfide. (Zhang, Skardal and Prestwich 2008) Poly (lactic acid) (PLA), poly (glycolic acid) (PGA), and poly caprolactone (PCL) are common hydrolytically degradable blocks, which have been used to synthesize triblock (ABA) polymers by ring opening polymerization. These triblock polymers have been further terminated with acrylates to form PLA-PEG-PLA diacrylate and PGA-PEG-PGA diacrylate. (Sawhney, Pathak and Hubbell 1993; Burdick, Mason, Hinman, Thorne and Anseth 2002; Ifkovits and Burdick 2007) In order to enhance the degradation of the ester bonds linked to PEG chains in the hydrogel structure, thiol-acrylate reaction has also been used. (Jo, Gantz, Hubbell and MP 2009; Hudalla, Eng and Murphy 2008; Rydholm, Anseth and Bowman 2007; Rydholm, Bowman and Anseth 2005; Nuttelman, Tripodi and Anseth 2005; Nuttelman, Rice, Rydholm, Salinas, Shah and Anseth 2008).

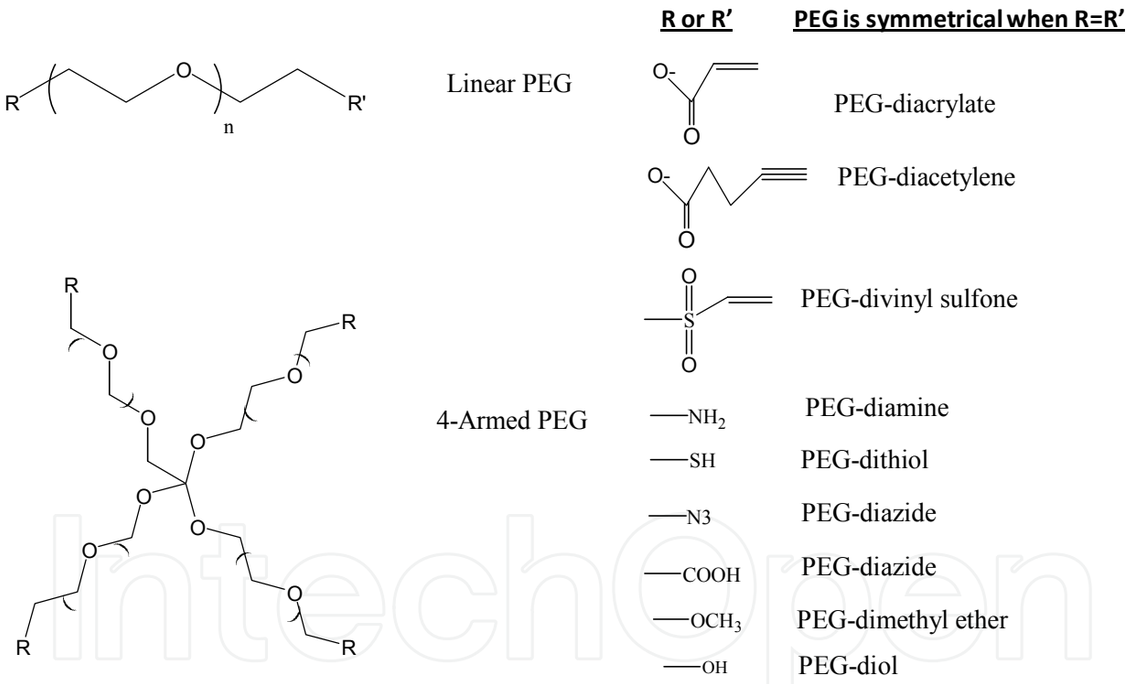

Scheme 1. Linear PEG and 4-armed PEG structures with various possible functional end groups.

PEG hydrogels are attractive as scaffolds, because they provide 3D environment for tissue regeneration. The limitation of PEG hydrogels on the other hand, is that they exhibit no biological activity, because PEG chains are not adhesive by their nature. (Lee, Lee and Andrade 1995) In order to mimic the natural extracellular matrix (ECM), researchers developed various types of biofunctional PEG hydrogels. (Lutolf 2009; Cushing and KS 2007; Lutolf and Hubbell 2005; Tibbitt and Anseth 2009) The components in the natural ECM is crucial in mediating cell functions, and possess critical role such as cell adhesion,

proteolytic degradation, and growth factor binding. (Badylak 2002; Badylak 2007) Various strategies have been used to tether ECM-derived biological molecules to PEG hydrogel structure, which provided fundamental knowledge to understand ligand incorporation within PEG hydrogels as well as cell/scaffold interactions. (Lutolf and Hubbell 2005; Cushing and KS 2007) Various cell lines including fibroblasts, chondrocytes, vascular smooth muscle cells (SMCs) and endothelial cells (ECs), osteoblasts, neural cells, and stem cells have been studied to observe their immobilization on biofunctional PEG hydrogels. (Lutolf and Hubbell 2005; Tibbitt and Anseth 2009) In order to regulate specific cellular responses for tissue formation, control of biomolecule concentration, spatial incorporation, and distribution within PEG hydrogels have been investigated. (Ma 2008; Ksihara, Matsumura and Fisher 2008; Ifkovits and Burdick 2007; Shin, Jo and Mikos 2003; Liao, Chan and Ramakrishna 2008; Sands and Mooney 2007)

This chapter addresses the recent progresss in the modeling of biofunctional PEG hydrogel scaffolds which can be utilized for the development of biofunctional PEG hydrogels as tissue engineering scaffolds. The chapter begins with a discussion of the structure and function of the natural ECM model, and then highlights the ECM derived ligands that have been used to synthesize biofunctional PEG hydrogels, followed by current approaches for the development of mathematical models for PEG hydrogels, which can be used to control specific cues, such as cell adhesion and function, and growth factor binding.

2. ECM as a natural model:

Natural ECM has been used as a model for designing biomimetic scaffolds as a result of rapid increase in the development and understanding of matrix biology. In the human body, tissues contain significant extracellular space and ECM molecules are secreted by the cells into this space and form a complex network. The function of ECM is to provide mechanical support for tissues, to organize cells into tissues, and to control cell behaviour (Scheme 2).

Proteins and glycans are the two classes of biomacromolecules that make up the natural ECM. (Rhodes and Simons 2007; Gailit and Clark 1994) The tensile strength to the ECM is provided by collagen and elasticity by elastin, both of which are structural fibrous proteins. (Gailit and Clark 1994; Ottani, Raspanti and Ruggeri 2001; Rhodes and Simons 2007) Type I and Type II that possess a fibrillar structure are two of the many types of collagen (Celse, Poschl and Aigner 2003). Type I collagen is found in skin, bone and tendons, while Type II collagen is what gives cartilage its tensile strength. (Brodsky and Ramshaw 1997; Kuhn 1985) Found specifically in basal lamina, Type IV collagen forms networks. (Kuhn 1994) Laminin (LN) and fibronectin (FN) are adhesive proteins that bind cells to the ECM. LN, with its cross-shaped trimer structure, provides binding sites for membrane receptors, Type IV collagen, heparan sulfate proteoglycan (HSPG) and entacin as the major adhesive protein in basal lamina (Aumaille and Smyth 1998; Beck, Hunter and Engel 1990; Gole and Pohl 2002; Kumagai, Okano and Kitagawa 2000). The many binding domains of FN, a V-shaped dimer, facilitate the connection between the ECM and cell membrane (Potts and Campbell 1994), in addition to binding proteins and cell-surface receptors. (Johansson, Svineng, Wennerberg, Armulik and Lohikangas 1997; Potts and Campbell 1994) Glycosaminoglycans (GAGs) and proteoglycans (PGs) are the glycans that make up the highly negatively charged, gelatinous ground substances rich in polysaccharide and in which the ECM proteins are embedded. (Horkay, 2008; Papagiannopoulos 2008; Rhodes 2007; Scott 1995) Sulfated GAGs, such as chondroitin, dermatan, heparan and keratin sulfates, that can

assemble on proteins rich in serine to form PGs and non-sulfated ones like hyaluronic acid (HA) are the two types of GAGs which are linear polymers of repeated disaccharide derivative. (Dudhia 2005; Luo, Guo, Zheng, Chen, Wang and Vertel 2000; Vertel 1995) Molecular signaling and nutrient diffusion are facilitated by glycans. When tissues are under pressure, GAGs and PGs prevent tissue collapse to some extent by absorbing compressive stresses because they swell in the aqueous environment between protein fibrils.

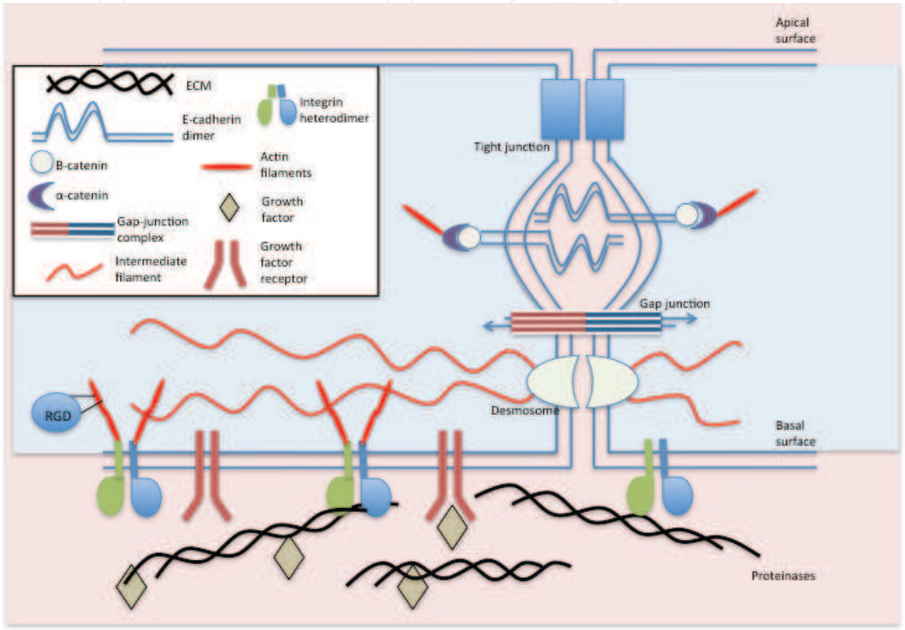

Scheme 2. Model of cell-extra cellular matrix (ECM) interactions.

Cell adhesion, proteolytic degradation and growth factor (GF)-binding are the three basic biofunctions of the ECM. Forming complex 3D networks by self-assembly or cell-directed assembly, (Traub 1978; Obrink, Laurent and Carlsson 1975; Guidetti, Bartolini, Bernardi, Tira, Berndt, Balduini and al. 2004; Zhu, Latridis, Hlibczuk, Ratcliffe and Mow 1996) the ECM components provide an environment for cell receptors to bind. Following this binding, the role of a cell in a tissue is determined by gene and protein expression which is affected by a series of intracellular enzymatic reactions initiated by these receptor-ligand interactions. (Cukierman, Pankov and Yamada 2002) Meanwhile, the microenvironment of the cells is formed and degenerated by the signals from these cells. Hence, the ECM has the role of providing a bioactive and dynamic environment for cellular functionality, in addition to filling up the extracellular space as a mechanical scaffold. (Rhodes and Simons 2007)
Most functions of the cell such as cell proliferation and cell migration can occur only after the cell's attachment to the ECM. (Jensen and Host 1997; Huttenlocher, Sandborg and Horwitz 1995; Humphries and Newham 1998) Many cell-surface receptors, such as integrins, selectins, CD44 and syndecan,(Cohen, Joester, Geiger and Addadi 2004; Henricks and Nijkamp 1998; Woods, Oh and Couchman 1998; Woods and Couchman 1998) are served cell-adhesive domains by the ECM. Integrins are responsible for cell anchorage and signal trigger through attachment to the ECM that lead to cell functioning, cell-cycle progression and different phenotype expression; (Woods, Oh and Couchman 1998; Ruoslahti and Pierschbacher 1987; Haas and Plow 1994; Katz, Zamir, Bershadsky, Kam,

Yamada and Geiger 2000; Webb, Parsons and Horwitz 2002) therefore they play an important role in tissue development, organization and maintenance by binding to the functional cell binding domains in the ECM such as FN, LN and collagen. (Chen, Chang, Gilson 2006; Woods, Couchman 2000)

A number of biological processes, such as cell migration, tissue repair and remodeling are actuated by the proteolytic degradation of the natural ECM. (Ellis and Murphy 2001; Murphy and Gavrilovic 1999; Murphy, Knauper, Atkinson, Gavriliovic and Edwards 2000) There are specific clevage sites on collagen, fibrin, FN, LN and other ECM proteins for degradation by enzymes such as matrix metalloproteinasas (MMPs), plasmin and elastase. (Seiki 2002; Chang and Werb 2001; Giannelli, Falk-Marzillier, Schiraldi, Stetler-Stevenson and Quaranta 1997; Ogura, Matsunaga, Nishiyama and Amano 2008; Mydel, Shipley, Adair-Kirk, Kelley, Broekelmann and Mecham 2008) Collagenases gelatinases, stromelysins, matrilysins, and membrane-type MMPs, which are made up of several domains including propeptide, catalytic, and hemopexin (except for matrilysin) domains, and are responsible for the degradation of collagens, proteoglycans, and various glycoproteins, (Turk, Huang, Piro and Cantley 2001; Nagase and Fields 1996) the five families of cell-secreted MMPs, which are endo-peptidases dependent on zinc and involved in the remodeling of the ECM, have effect on morphogenesis, angiogenesis, arthritis, skin ulcer, tumor invasion and metastasis. (Amano, Akutsu, Matsunaga, Kadoya, Nishiyama, Champliaud and al. 2001) MMPs, inactive zymogens as secreted, need to be activated in order to function. Tissue inhibitors of metalloproteinase's (TIMPs) regulate the activity of MMPs in the post-transcriptional stage; therefore regulated degradation to delineate the cellular environment is performed by MMPs and TIMPs. (Amano, Akutsu, Matsunaga, Kadoya, Nishiyama, Champliaud and al. 2001; Nagase and Fields 1996; Turk, Huang, Piro and Cantley 2001)

Binding to the ECM controls the stability, activity, release and spatial localization of growth factors (GFs), proteins that regulate gene expression and cell functions like differentiation, migration and proliferation depending on the conditions of the cell environment, (Silva, Richard, Bessodes, Scherman and Merten 2009; Babensee, McIntire and Mikos 2000) during the natural tissue development. (Zisch, Lutolf and Hubbell 2003) When they are in contact, ECM proteoglycans are associated with GFs, including fibroblast growth factor (FGF), transforming growth factor (TGF), epidermal growth factor (EGF), vascular endothelial growth factor (VEGF) and platelet-derived growth factor (PDGF), in order to provide integrations and eliminate immediate dispatch.

3. Bioactive modification of ECM-mimic

The scaffolds in tissue engineering should be able to perform cell-specific adhesion and promote the motion of signaling biomolecules, in addition to being biocompatible, biodegradable, highly porous and not prone to causing immunogenic reactions. Although PEG hydrogels are preferred in designs that require flexibility and porosity similar to cartilage, they are not optimum in supplying the cells with the environment they need due to PEG's inability to adhere to cells and not being biodegradable. The addition of bioactive materials such as cell adhesive peptides (CAPs), enzyme-sensitive peptides (ESPs) and growth factors is necessary to obtain the similar biofunction of ECM such as specific cell adhesion, enzyme-sensitive degradation and GF-binding, respectively; because addition of segments like PLA and PGA, which are hydrolytically open to change, is not enough to increase biodegradability.

Biofunctions of the ECM like cell binding, proteolytic degradation and GF-binding are often chemically accomplished by short peptide sequences present in collagen, elastin, FN, LN and PGs. (Mel, Jell, Stevens and Sefalian 2008; Heino 2007; Mineur, Guignandon, Lambert, Lapiere and Nusgens 2005; Luzak, Golanski, Rozalski, Boncler and Watala 2003; Pocza, Suli-Vargham, Darvas and Falus 2008; Girotti, Reguera and Rodriguez-Cabello 2004; Nomizu, Weeks, Weston, Kim, Kleinman and Yamada 1995; Fosang, Last, Knauper, Murphy and Neame 1996; Ruoslahti 2003; Leahy, Aukhil and Erickson 1996; Lin, Takahashi, Liu and Zamora 2006) PEG hydrogels are modified with these ECM-derived short peptides,(Shin, Jo and Mikos 2003) proteins(Hynd, Frampton, Dowell-Mesfin, Turner and Shain 2007; Halstenberg, Panitch, Rizzi, Hall and Hubbell 2002; Nie, Akins and Kiick 2009; Moon, Lee and West 2007) or proteoglycans. (Bryant, Arthur and Anseth 2005; Li, Williams, Sun, Wang, Leong and Elisseeff 2004; Masters, Shah, Walker, Leinwand and Anseth 2004; Khetan, Katz and Burdick 2009) Short peptide sequences are more stable, easier to synthesize and harder to denature or degrade than the entire protein structure. (Massia and Hubbell 1992) Reactive groups such as acrylate, amine, thiol, azide, maleimide and bitin/streptavidin have been used in order to bind ECM-derived biomolecules covalently into PEG hydrogel networks.

4. Bioactive molecules for biofunctional PEG hydrogel

The following sections summarize different types of biofunctional PEG hydrogels which have been synthesized through incorporation of biomolecules.

Cell adhesion bearing sites in PEG Hydrogels

Inability of PEG hydrogels to perform cell specific adhesion is a major limitation in tissue engineering. A variety of cell adhesive peptides (CAPs), mainly derived from four ECM proteins, FN (e. g. , RGD, KQAGDV, REDV and PHSRN), LN (e.g., YIGSR, LGTIPG, IKVAV, PDGSR, LRE, LRGDN and IKLLI), collagen (e.g., DGEA and GFOGER) and elastin (e.g., VAPG) have been used for modifying PEG hydrogels. RGD peptides, whose cell binding domains are derived from FN, LN and collagen, are most commonly used modifications. (Hersel, Dahmen and Kessler 2003; Ruoslahti 2003) While linear RGD peptides inrease the affinity for cell binding, (Leahy, Aukhil and Erickson 1996) cyclic RGD (cRGD) peptides increase biological activity up to 240 times compared to linear ones. (Haubner, Schmitt, Holzemann, Goodman, Jonczyk and Kessler 1996; Haubner, Gratias, Diefenbach, Goodman, Jonczyk and Kessler 1996; Locardi, Mullen, Mattern and Goodman 1999; Kaufmann, Fiedler, Junger, Auernheimer, Kessler and Weberskirch 2008) A better mimic of RGD loop structure and enhanced cell specific adhesion in PEG hydrogels have been achived by the incorporation of cRGD peptides. (Zhu, Tang, Kottke-Marchant and Marchant 2009)

Enzymatically-responsive PEG Hydrogels

It is important that the degradation rate of scaffolds matches the new tissue regeneration at the defect site. More rapid degradation than tissue regeneration will cause the scaffolds to lose their carrier function for cell growth, whereas slower degradation than tissue regeneration will decrease the efficiency of tissue regeneration. Although PEG hydrogels have ester bonds that can be hydrolized, this degradation is not fast enough both in vitro and in vivo. Incorporation of polyester segments such as PLA and PGA promotes hydrolytic degradation of PEG hydrogels; however, the process stays non-responsive to cellular signals or cell-secreted enzymes. Incorporation of enzyme-sensitive peptide (ESP) sequences for proteolytic degradation is the best way to accomplish biodegradability. Cell adhesion to PEG hydrogels have also been modulated by such enzyme-sensitive designs.

Growth-factor Binding PEG Hydrogels

Growth factors (GFs), which are polypeptides that transmit signals to operate cellular activities, have short half-lives in free forms or in the circulation and need to bind to matrix molecules for activity and stabilization. Binding to the receptors on the surface of target cells is what initiates their action. Cell functions and tissue formation are guided by binding of GFs to proteoglycans. (Zisch, Lutolf and Hubbell 2003) GFs are best incorporated in PEG hydrogels during the formation of the gel; however, rapid burst release during the initial swelling phase can be observed with this direct loading method. (Burdick, Mason, Hinman, Thorne and Anseth 2002) It is hard to control this mechanism since the rate of protein release is diffusion-controlled within a hydrogel. Two major strategies, covalent attachment and specific interaction, have been developed to mimic the GF-binding function of the ECM in PEG hydrogels. GFs have been modified with several functional groups for covalent attachment. Besides this modification, GF-binding hydrogels is another approach in delivering GFs. This method prevents potential damage to GFs during covalent modification and therefore biological activity of GFs can be maintained during release period. Chemical modification of heparin, chondroitin sulfate (CS) and hyaluronic acid (HA) with various reactive groups, such as acrylate, thiol, or maleimide, followed by reacting with the functionalized derivatives of PEG or multiarm PEG to form GAG-bearing PEG hydrogels by carboxyl/amine conjugation, copolymerization, Michael addition, and specific interaction between heparin and GFs or heparin binding peptides (HBPs) have been the central efforts to develop this mechanism. (Cai, Liu, Zheng and Prestwich 2005; Yamaguchi, Zhang, Chae, Palla, Furst and Kiick 2007; Zhang, Furst and Kiick 2006) Thiol-acrylate photopolymerization to incorporate thiol-containing biotin into PEG hydrogels for specific interaction with strepavidin-modified GFs like bFGF is another method to make GF-binding PEG hydrogels. (Lin and Anseth 2009; Zhu 2010)

Immunoisolation with PEG Hydrogels

Additional challenges come up in controlling the function and survival of cells encapsulated in PEG hydrogels during the transition between *in vitro* to *in vivo* studies. Although PEG hydrogels can act as a barrier between the encapsulated cells and the immune or inflamatory cells, small cytotoxic molecules like reactive oxygen species (ROS) and pro-inflammatory cytokines, such as tumor necrosis factor-a (TNFa, 17. 4 kDa) and interleukin-1b (IL-1b, 17 kDa) can still diffuse through the gel. Apoptosis or impaired cell function can result from the penetration of these molecules into the hydrogel. A polymerizable superoxide dismutase (SOD)-mimetic macromer, tetraacrylate of Mn(III)tetrakis(1-methyl-4-pyridyl) porphyrin pentachloride (MnTMPyP), have been synthesized and copolymerized with PEGDA to form hydrogel networks that provide SOD-mimetic activity to protect encapsulated cells from ROS-mediated damage. (Cheung, McCartney and KS 2008) Immobilizing cytokine-antagonizing antibodies like anti-Fas MAb (binding to the Fas antigen of Jurkat T cells) in PEG hydrogels has been another attempt; however, the large size for conjugation, poor stability and immunogenicity have been the concerns for this method. (Cheung and KS 2006)

Drug Delivery from PEG Hydrogels

Critical properties of PEG hydrogels like good biocompatibility, non-immunogenity and resistance to protein adsorption makes them an important type of hydrophilic polymers that can be used for drug delivery. (Lee, Lee and Andrade 1995; Alcantar, Aydil and Israelachvili 2000) An example of this is pressure-sensitive adhesive hydrogel matrix based on a poly-complex between poly(N-vinylpyrrolydone) (PVP) and oligomeric PEG which has been

designed to enhance transdermal drug delivery (Feldstein et al. 1997; Feldstein, Plate, Sohn, Voicu and protection 1999; Feldstein, Tohmakhchi, Malkhazov, Vasiliev and Plate 1996).

5. Free radical copolymerization for bioactive modification of PEG hydrogels

PEG hydrogels from PEGDA macromers have been made with the method of free radical polymerization (FRP), especially photopolymerization where photoinitiators are present. In order to make biofunctional PEG hydrogels, copolymerization of acrylated biomolecules have been performed to incorporate bioactive molecules into PEG hydrogel networks. Copolymerization with peptide monoacrylates or diacrylates and thiol-acrylate photopolymerization are the common methods used for this strategy.

In order to make bulk cell-adhesive hydrogels, PEGDA can be copolymerized with monoacrylates of CAPs. By functionalizing the N-terminal amines of RGD peptides with N-hydroxyl succinimide (NHS) ester of acrylic acid (AA-NHS) and acryloyl-PEG-NHS (Acr-PEG-NHS, Mw 3400) to produce mono-acrylamidoyl RGD (RGD-MA) and RGD-PEG monoacrylate (RGD- PEGMA), monoarcylated RGD with or without PEG spacers can be synthesized, respectively. (Hern and Hubbell 1998) As a result, cell-adhesive hydrogels can be made by the copolymerization of RGD-MA or RGD-PEGMA monomers with PEGDA upon photopolymerization. Having a PEG spacer, PEGDA hydrogels with RGD-MA can spread the cells specifically. Several cell lines, such as fibroblasts, chondrocytes, vascular endothelial cells (ECs), osteoblasts, neural cells, and stem cells, have been observed to immobilize on bioactive PEG hydrogels. (Lutolf 2009; Nuttelman, Rice, Rydholm, Salinas, Shah and Anseth 2008)

Using peptide monoacrylates in this method results in random distribution of RGD peptides in hydrogels. In addition, hydrogel formation and its mechanical properties are limited due to the limitations in peptide incorporation in the hydrogel when monoacrylates are used. Creating a peptide-containing PEGDA macromer like RGD-PEGDA with RGD attached to two PEG monoacrylates, which has a similar structure to PEGDA with two C-C double bonds for polymerization is a method to control cell behavior. (Zhu, Beamish, Tang, Kottke-Marchant and RE 2006) This way, the spatial organization of peptide ligands in hydrogels can be controlled and the effort of peptide incorporation can be eliminated. Enzyme-sensitive peptide (ESP)-containing PEGDA (ESP-PEGDA), another important type of peptide-modified PEG diacrylates, has a different structure than that of CAP-PEGDA. With its two reactive groups on both ends for conjugation with Acr-PEG-NHS, ESP is inserted between two PEG monoacrylate (PEGMA) chains, whereas a CAP with two amines on one end for attachment as a pendant on the PEGDA chain synthesizes CAP-PEGDA. Proteolytic degradation of the natural ECM by specific enzymes, such as plasimin, elastase and MMPs, is mimicked by ESP-PEGDA for photopolymerization to form hydrogels. Also, bioactive PEG hydrogels with dual biofunctions like enzyme-sensitive degradation and specific cell adhesion can be made by the copolymerization of ESP-PEGDA with cell-adhesive PEG macromers like RGD-PEGMA. (Patel, Gobin, West and Patrick 2005; Lee, Moon, Miller and West 2007; Gobin and West 2003)

The molecular weight of polymers created by free radical polymerization (FRP) is controlled by thiol-containing compounds used as chain transfer reagents. Cysteine-containing peptides are expected to play a similar role as chain transfer reagents in the FRP of PEGDA, which leads to the incorporation of cysteine-containing peptides into the PEG hydrogel network. (Reddy, Cramer and Bowman 2006; Cramer, Reddy, O'Brien and CN 2003; Cramer

and Bowman 2001; Houllier and Bunel 2001) Thiol-acrylate photopolymerization can be utilized to bioactively modify PEG hydrogels as an alternative approach. (Polizzotti, Fairbanks and Anseth 2008; DeForest, Polizzotti and KS 2009; Salinas and KS 2008; Salinas and Anseth 2008) Stoichiometric ratios, polymerization time and pH are not limitations for this method and it results in a robust, cost-efficient and cytocompatible reaction scheme for the incorporation of peptide sequences into PEG hydrogels for 3D cell culture and directing cellular function. (Salinas and Anseth 2008)

6. Mathematical models for the prediction of PEG hydrogel membrane properties for biological applications

Recent studies have provided evidence that it is important to control the swelling ratio, diffusion rate, and mechanical properties of a crosslinked polymer in the design of PEG hydrogels for biomedical applications. (Elliott, Anseth and Bowman 2001) It has also been shown that, polymer synthetic peptide epitopes might be useful, specifically in the design of an ECM mimic to promote tissue survival and function. (Weber, Hayda and Anseth 2008; Weber and Anseth 2008; Weber, Hayda, Haskins and Anseth 2007) Thickness and permeability of the membrane, as well as the level of peptide incorporation within the membrane, are all critical factors that determine the success of immunoprotective devices and tissue function. These are crucial because a thick membrane can present a large diffusion barrier to oxygen, nutrient, metabolites, and/or the therapeutic agent released by the cell, yet a very thin barrier is more likely to have defects that may expose the transplanted cells to the immune system of the host. (Ji, Childs and Mehta 2001) Development of a biofunctional PEG hydrogel requires the control of ligand concentration which is important to direct the desired signaling pathways. (West 2005) For example, microencapsulation via surface initiated photopolymerization of PEG hydrogel is one method to make microcapsules around cells or islets. (Pathak, Sawhney and Hubbell 1992) Release of the insulin through the membrane capsule and the viability of the encapsulated islets after transplantation depend on the structure and the thickness of the capsule. Experimentally, a variety of parameters such as the chemical composition of the photopolymerization system, the duration of photopolymerization and the intensity of the excitation light source have been found to affect the gel thickness(Cruise, Hegre, Scharp and Hubbell 1998) and permeability characteristics of the capsule wall. (Cruise, Scharp and Hubbell 1998) In previous studies, Kızılel *et al.* developed experimental and mathematical models to describe the details of the complex process of PEG hydrogel and biofunctional PEG hydrogel formation which were based on an understanding of the individual fundamental steps of the photopolymerization process. (Kizilel, Sawardecker, Teymour and Perez-Luna 2006; Kizilel, Perez-Luna and Teymour 2009; Kizilel, Perez-Luna and Teymour 2006; Kizilel, Perez-Luna and Teymour 2004; Kizilel 2010; MacDonald, El-kholy, Riedel, Salapatek, Light and MB 2002) Those models greatly improved our understanding of such a complex polymerization system and provided important information on the effect of parameter variation (e. g. monomers or initiator concentration, light intensity, duration of photopolymerization) on properties of the membrane such as thickness, crosslink density, gelation, and the distribution of biological ligands within the hydrogel as these variables are changed. These models not only lead to better optimization strategies based upon numerical simulations of parameter variation such as monomer, light intensity, duration of photopolymerization, but also give further insights into the hydrogel properties at the

microscopic level that cannot be obtained through experimental observations such as the presence of gradients in peptide incorporation, crosslink density, the evolution of these gradients with time and the early stages of hydrogel formation.

Model Description

The process of hydrogel membrane formation by free radical copolymerization of PEG-DA VP, and acrl-PEG-GLP-1 involves excitation of surface bound eosin to its triplet state as a result of irradiation with green light (514 nm). (Valdes-aguilera, Pathak, Shi, Watson and Neckers 1992) Electron transfer and proton loss from the triethanolamine to the excited eosin results in the formation of the neutral α-amino radical (TEA•), which initiates polymerization in this system. (Neckers, Hassoon and Klimtchuk 1996; Kumar and Neckers 1991) It must be noted that, in this polymerization process, the TEA• free radicals are generated at the cell-prepolymer interface and TEA• radicals will diffuse away from the surface, and initiate polymerization in a region that is in close proximity with the surface. The process of biofunctional PEG hydrogel membrane formation is a nonlinear polymerization process where a branched polymer chain is formed through propagation of a radical through the pendant double bonds present in PEG-DA chains. Excessive crosslinking occurs through pendant double bond (PDB) propagation followed by termination by combination. Since crosslinking leads to the formation of a very large molecule of infinite molecular weight, complicated solution techniques are required to mathematically describe gel formation.

In previous studies, Kızılel et al. described the branching characteristics and crosslinking mechanism in PEG-DA/VP copolymerization that lead to gel formation, and the method of moments(Bamford and Tompa 1954) along with the pseudo-kinetic rate constant approach(Hamielec and MacGregor 1983) has been applied to develop a mathematical model for the process of islet encapsulation within biofunctional PEG hydrogel through interfacial photopolymerization. (Kizilel, Perez-Luna and Teymour 2006; Kizilel 2010) In those models, new features are also included; concentration dependent propagation of VP monomer, and the reaction diffusion termination for all monomers. In order to derive the kinetic model, several assumptions such as monoradical assumption, and the diffusion of vinyl pyrrolidone through the newly formed hydrogel were made about the copolymerization system. As the polymerization proceeds, capsule starts to form on the surface. Since the thickness varies with time, this becomes a moving boundary problem. The growth of the membrane occurs as a result of reaction of monomers at the membrane surface.

The polymerization system consists of initiation, propagation, chain transfer to TEA, radical termination by combination and reaction through pendant double bond steps. It is also assumed that the terminal model of copolymerization is applicable and termination by disproportionation step is not included. The process involves the copolymerization of *A (VP), B (PEG-DA)* and C (acrl-PEG-GLP-1) whose elementary reactions are shown below. The symbols *A*, B**, and *C** are used to indicate the type of monomer unit at the chain end identity of the propagating radical. These denote VP, PEG-DA and acrl-PEG-GLP-1 respectively.

Initiation:

In this step the initiator radical (R_{in}), which was also called α-amino radical in this system, forms as a result of its reaction with eosin Y and reacts with the monomers to form live radicals of length one.

$$Y_{ac} \underset{k_{-1}}{\overset{\nu k_1}{\Leftrightarrow}} Y^* \nu K \tag{1}$$

$$Y^* + TEA \rightarrow Y_{in} + R_{in} \bullet \mathrm{k_f} \tag{2}$$

$$R_{in} \bullet + A \rightarrow A_1 \bullet \mathrm{k_{i1}} \tag{3}$$

$$R_{in} \bullet + B \rightarrow B_1 \bullet \mathrm{k_{i2}} \tag{4}$$

$$R_{in} \bullet + C \rightarrow C_1 \bullet \mathrm{k_{i3}} \tag{5}$$

where $\nu K = \nu \frac{k_1}{k_{-1}}$, K is the equilibrium constant for excitation and, νK represents the amount of excitation radiation absorbed by eosin Y molecules. Thus, ν would take into account the intensity of the light source because an increase of excitation intensity would result in a larger number eosin molecules excited to the triplet state.

Propagation:

Propagation of the three monomers, *A (VP), B (PEG-DA),* and *C (acrl-PEG-peptide)* leads to three types of propagating species, one with *A* at the propagating end, one with *B* at the propagating end, and the other with C at the propagating end. These are represented by *A*, B*,* and *C**. This classification is made because the reactivity of the propagating species is dependent on the monomer unit at the end of the chain. (Odian 2004; Dotson, Galvan, Laurence and Tirrell 1996) Radical chains of length j react by adding monomer units to the polymer chain to form longer radical chains of length j+1 according to the following mechanism:

$$A_j \bullet + A \rightarrow A_{j+1} \bullet \mathrm{k_{p11}} \tag{6}$$

$$A_j \bullet + B \rightarrow B_{j+1} \bullet \mathrm{k_{p12}} \tag{7}$$

$$A_j \bullet + C \rightarrow C_{j+1} \bullet \mathrm{k_{p13}} \tag{8}$$

$$B_j \bullet + A \rightarrow A_{j+1} \bullet \mathrm{k_{p21}} \tag{9}$$

$$B_j \bullet + B \rightarrow B_{j+1} \bullet \mathrm{k_{p22}} \tag{10}$$

$$B_j \bullet + C \rightarrow C_{j+1} \bullet \mathrm{k_{p23}} \tag{11}$$

$$C_j \bullet + A \rightarrow A_{j+1} \bullet \mathrm{k_{p31}} \tag{12}$$

$$C_j \bullet + B \rightarrow B_{j+1} \bullet \mathrm{k_{p32}} \tag{13}$$

$$C_j \bullet + C \rightarrow C_{j+1} \bullet \mathrm{k_{p33}} \tag{14}$$

Termination:
Termination by combination reaction leads to the formation of longer dead polymer chains. Termination by combination reaction must be taken into account because it also leads to branching and gelation.

$$A_j \bullet + A_p \rightarrow P_{j+p}\, \mathrm{k_{tc11}} \tag{15}$$

$$A_j \bullet + B_p \rightarrow P_{j+p}\, \mathrm{k_{tc12}} \tag{16}$$

$$A_j \bullet + C_p \rightarrow P_{j+p}\, \mathrm{k_{tc13}} \tag{17}$$

$$B_j \bullet + B_p \rightarrow P_{j+p}\, \mathrm{k_{tc22}} \tag{18}$$

$$B_j \bullet + C_p \rightarrow P_{j+p}\, \mathrm{k_{tc23}} \tag{19}$$

$$C_j \bullet + C_p \rightarrow P_{j+p}\, \mathrm{k_{tc33}} \tag{20}$$

Chain Transfer to TEA:
The radicals can also react with the chain transfer agent, TEA. In this case the growing radical is transferred to TEA, which hinders the growth of a polymer chain while at the same time generating a free radical capable of starting the growth of another polymer chain as follows:

$$A_j \bullet + TEA \rightarrow P_j + R_{in} \bullet\, \mathrm{k_{tr1}} \tag{21}$$

$$B_j \bullet + TEA \rightarrow P_j + R_{in} \bullet\, \mathrm{k_{tr2}} \tag{22}$$

$$C_j \bullet + TEA \rightarrow P_j + R_{in} \bullet\, \mathrm{k_{tr3}} \tag{23}$$

Reaction through a Pendant Double Bond:
When a newly formed radical reacts through a pendant double bond, a quaternary branch point is created.

$$A_j \bullet + P_p \rightarrow B_{j+p} \bullet\, \mathrm{k^*_{p12}} \tag{24}$$

$$B_j \bullet + P_p \rightarrow B_{j+p} \bullet\, \mathrm{k^*_{p22}} \tag{25}$$

$$C_j \bullet + P_p \rightarrow B_{j+p} \bullet\, \mathrm{k^*_{p32}} \tag{26}$$

Membrane thickness:
The equation describing the increasing size of the polymer membrane can be formulated as:

$$\varphi_p \rho_{polymer} \frac{dv}{dt} = v \left[-\left.\frac{d[A]}{dt}\right|_{r_m} MW_{VP} - \left.\frac{d[B]}{dt}\right|_{r_m} MW_{PEG} - \left.\frac{d[C]}{dt}\right|_{r_m} MW_{PEG-pep} \right] \tag{27}$$

where $\rho_{polymer}$ is polymer density (g. L^{-1}), MW_{PEG}, MW_{VP}, and $MW_{PEG\text{-}pep}$ are the molecular weights of PEG-DA, VP, and acrl-PEG-GLP-1 respectively, dv/dt represents volume growth rate of the hydrogel membrane, $dv = Sdr$, and S is the surface area of the capsule. The equation can be written in general form as:

$$\frac{dr}{dt} = \frac{r}{a\varphi_p \rho_{polymer}} \left[-\frac{d[A]}{dt}\bigg|_{r_m} MW_{VP} - \frac{d[B]}{dt}\bigg|_{r_m} MW_{PEG} - \frac{d[C]}{dt}\bigg|_{r_m} MW_{PEG-pep} \right] \quad (28)$$

and a is equal to 3 for the case of spherical model (islet is assumed to be perfectly spherical), and it is equal to 1, for the case of rectangular coordinates. Mass growth rate of the polymer capsule is related to the consumption of monomers *A, B*, and *C*, and φ_p represents the volume fraction of the polymer chains in the water swollen hydrogel. Molecular weights of *PEG-DA*, *VP*, and *acrl-PEG-peptide* are 3400, 111. 43, and 6754. 67 g. mol^{-1} respectively.

Boundary Conditions:

As stated earlier, it was assumed that the VP monomer and the initiator radicals could diffuse through the newly formed hydrogel. This imposes the following boundary conditions in this model:

$$\frac{\partial[A]}{\partial r}\bigg|_{cell\ surface} = 0 \quad (29)$$

i. e. , VP cannot diffuse into the cell or through the solid surface.

The rate of formation of initiator free radicals at the surface is given by its rate of formation by electron transfer from TEA to excited eosin Y, plus its consumption with the monomers of type *A, B*, and *C* to form live radicals of length one, plus its formation through the reaction of live radicals with TEA, plus its outward diffusion.

$$\frac{\partial[R_{in}]}{\partial t}\bigg|_{cell\,surface} = \left[\begin{array}{l} k_{in}\left([Y_{tot}]-[Y_{in}]\right)TEA - \bar{k}_i[M][R_{in}] \\ \qquad + \bar{k}_{tr}[TEA][Y_0] + D_{R_{in}} \dfrac{a}{r} \dfrac{\partial[R_{in}]}{\partial r} \end{array} \right]_{r=r_0} \quad (30)$$

where r_o is the radius at the cell surface, a is equal to 3 for spherical coordinates and it is equal to 1 for rectangular coordinates. The predictions of membrane thickness for different concentrations have been done for rectangular coordinate system, when the comparisons were made with experimental observations. It has been observed that the predicted differences of thicknesses between rectangular and spherical coordinate system were not statistically significant, therefore spherical coordinate system have been used for the remaining thickness predictions.

Effects of VP and PEG-DA Concentrations on Membrane Thickness. The effects of PEG-DA and VP concentrations on the thickness of the hydrogel membrane and crosslink density demonstrated that VP and PEG-DA has a positive effect on the membrane thickness, and that higher PEG-DA and VP concentration results in thicker membranes. The positive effect of VP on thickness was explained by the effect of VP propagation (k_{p11}) and termination rate constants (k_{tc11}), which have been incorporated into the present model as a function of VP concentration as was suggested in previous recent studies. (Stach, Lacik, Chorvat, Buback,

Hesse, Hutchinson and Tang 2008; White, Liechty and Guymon 2007) Recently, Stach et al measured the propagation rate coefficient (k_{p11}) of N-vinyl pyrrolidone (NVP) in aqueous solution at a concentration range from 1. 8% to 100 wt % NVP via pulsed-laser polymerization-size exclusion chromatography method (PLP-SEC). (Stach, Lacik, Chorvat, Buback, Hesse, Hutchinson and Tang 2008) The authors observed that k_p increases toward lower NVP concentrations in water, and that k_{p11} is enhanced during polymerization to higher monomer conversion of a given aqueous solution of NVP. The pronounced increase of VP propagation rate constant, k_{p11}, toward lower VP concentrations in water was assigned to a genuine entropic effect. According to transition state theory (TS), the preexponential factor in the Arrhenius equation is determined by the geometry of the rotating groups in the reactants, and by the rotational potentials of the relevant internal motions in the TS. (White, Liechty and Guymon 2007; Heuts, Gilbert and Radom 1995) Large hindrance of rotational freedom is associated with significant entropy penalty, and this results in smaller Arrhenius constant (A), and propagation constant, k_p. When water molecules replace monomer molecules, the environment of the TS structure for the addition of a monomer molecule to a macroradical changes, which results in higher degree of rotational freedom at the chain end. As a result, k_p increases toward lower VP concentrations, and k_p is enhanced during polymerization to higher monomer conversion of a given aqueous solution of VP. (Stach, Lacik, Chorvat, Buback, Hesse, Hutchinson and Tang 2008)
Following formula correlates the relationship between k_p and concentration of NVP (C_{NVP}):

$$k_p = M_1 \upsilon_{rep} / (M_0 C_{NVP}) \tag{31}$$

where M_1 and ν_{rep} are the parameters measured in PLP experiments, M_0 and C_{NVP} represent molecular weight (MW_{VP}=111. 43 g. mol^{-1}) and concentration of NVP respectively. The relationship between propagation and termination rate constants of NVP has also been described recently in a separate study by White et al. ,(White, Liechty and Guymon 2007) where the authors investigated the importance of reaction-diffusion controlled termination in crosslinked acrylate/NVP copolymerization, and suggested that reaction diffusion termination, R, is expressed by:

$$R = \frac{k_t}{k_p M} \tag{32}$$

where M and R are the monomer double bond concentration, and reaction diffusion parameter respectively. In the recent biofunctional PEG hydrogel modeling study by Kızılel, the value of R has been taken as 25 L/mol, which was the value measured in NVP/diacrylate polymerization systems for conversions greater that 0. 2. (White, Liechty and Guymon 2007; Kizilel 2010) It was also considered that termination rate constants for PEG-DA and acrylate-PEG-GLP-1, k_{t22} and k_{t33}, are proportional with k_{p22} and k_{p33} respectively, with a proportionality constant of 30, as was measured previously. (Anseth, Wang and Bowman 1994; Anseth, Wang and Bowman 1994) The dependence of termination and propagation rate constants of VP on its concentration have also been incorporated into the model. VP is a common reactive diluent to photopolymerizable formulations, and is known to reduce the inhibition of free radical photopolymerization by atmospheric oxygen. It has been observed that for up to 45 double bond % NVP concentrations, NVP/diacrylate polymerizations are faster than that of bulk polymerizations of diacrylate. As a result of

positive contribution of VP on polymerization rates, thicker membranes were obtained as VP concentration in the prepolymer solution is increased.

The comparison of thicknesses for 25 % (w/v) PEG-DA condition ([acrl-PEG-GLP-1] = 14. 8 μM, [TEA]=225 mM) is illustrated in Figure 1 as thickness versus VP concentration for a total polymerization time of 150 seconds, where squares represent experimental measurements and line represents model simulation. As shown in Figure 1, a thickness of about 60 μm was reached at around 150 seconds of photopolymerization for a VP concentration of 37 mM. The thickness of the hydrogel membrane measured for the 25% (w/v) PEG-DA condition increases with VP concentration duration and reaches a limiting value of about 110 μm at around 592 mM VP concentration and becomes stationary at 110 μm at 592 mM VP for 150 seconds of polymerization time (Figure 1).

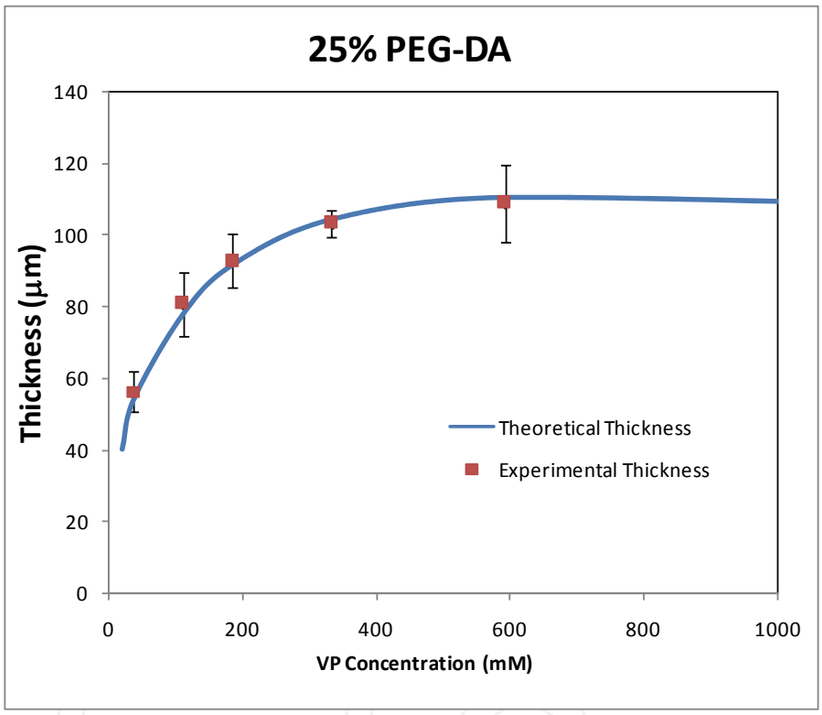

Fig. 1. The thickness of GLP-1 functionalized PEG hydrogel membrane versus VP concentration ([TEA]=225 mM, [acrl-PEG-GLP-1=14. 8 μM, photopolymerization time=150 seconds), and 25% PEG-DA in prepolmer solution. Squares denote experimental measurements and line represents model simulation.

The growth profile of the hydrogel membrane for various PEG-DA concentrations also demonstrated that increasing the concentration of PEG-DA in the prepolymer solution resulted in the formation of thicker membranes (Figure 2). The fact that the thickness of the resulting hydrogel was increased as the amount of PEG-DA in the precursor solution increased was consistent with previous observations. (Cruise, Hegre, Scharp and Hubbell 1998; Kizilel, Perez-Luna and Teymour 2006) The effect of PEG-DA concentration on thickness shows that, increasing PEG-DA concentration from 15% to 40 % (w/v) increases the membrane thickness by 40 μm for a total laser exposure time of 150 seconds ([acrl-PEG-GLP-1] =14. 8 μM, [TEA]=225 mM, [VP]=37 mM) (Figure 2).

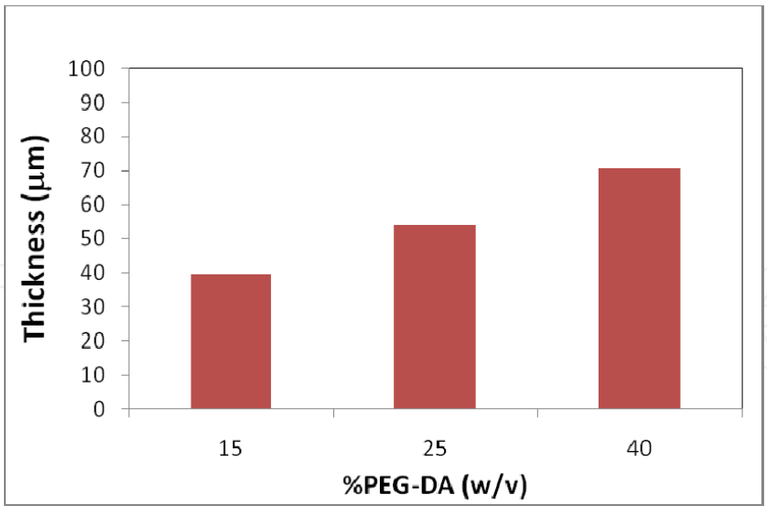

Fig. 2. Effect of % (w/v) PEG-DA in prepolymer on the thickness of GLP-1 functionalized PEG hydrogel membrane ([TEA]=225 mM, [acrl-PEG-GLP-1=14. 8 μM)

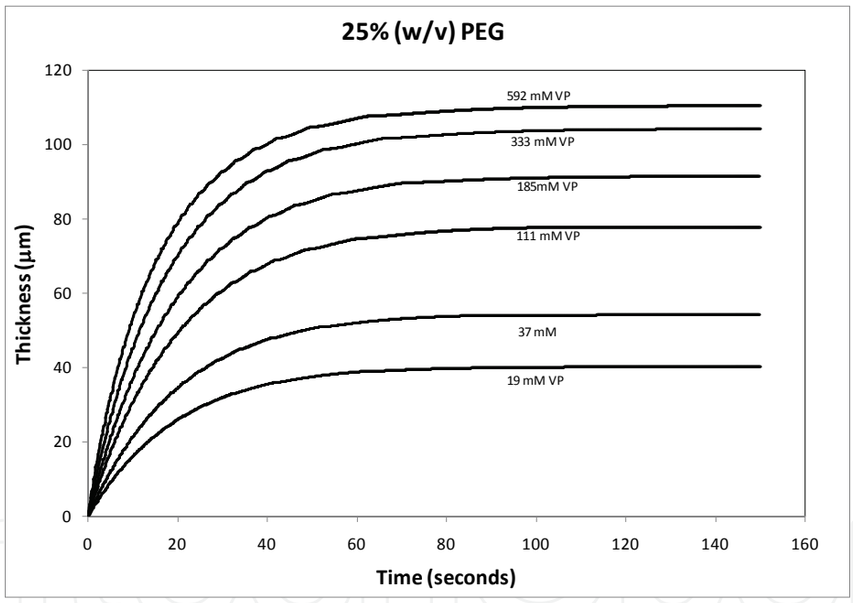

Fig. 3. Effect of concentration changes of VP on the thickness of GLP-1 functionalized PEG hydrogel membrane ([TEA]=225 mM, [acrl-PEG-GLP-1=14. 8 μM), and 25% (w/v) PEG-DA in prepolmer solution.

For all the conditions studied, the thickness of the hydrogel membrane increases rapidly with time during the early stages of photopolymerization, and then saturates to the maximum value (Figure 3). Therefore, once the saturation thickness is obtained, longer photopolymerization times would not result in higher membrane wall thickness. This was explained by the limited diffusion of photoinitiator through the newly formed hydrogel membrane. Higher thicknesses achieved for higher photoinitiator concentrations condition is caused by the formation and diffusion of more radical fragment (R_{in}) through the hydrogel membrane, which increases total amount of polymer (hydrogel) in the medium.

In addition to the comparison of thicknesses of the model and experiments, swelling experiments were used to confirm the capability of the model to capture dynamic features of experiments. Swelling ratios for 25% (w/v) PEG-DA concentration ([acrl-PEG-GLP-1] = 14. 8 μM, [TEA]=225 mM) and VP concentrations within the range of 19-592 mM is compared with the dimensionless crosslink density of the model (Figure 4). Crosslink density is a physical property related to the permeability of hydrogel. Therefore, high crosslink densities indicate that the permeability and swelling ratio of the hydrogel is low, whereas hydrogels with higher permeabilities and swelling ratios have lower crosslink densities. As shown in Figure 4, inverse of the swelling ratio has similar trend with the dimensionless crosslink density versus VP concentration. Both crosslink density and inverse of the swelling ratio increase up to a VP concentration of 185 mM, and VP concentrations beyond 185 mM does not increase the crosslink density and swelling ratio further. The comparisons of the results obtained for both thickness and swelling ratio proves that the model is valid to predict the thickness and permeability trends of this biofunctional PEG hydrogel polymerization process.

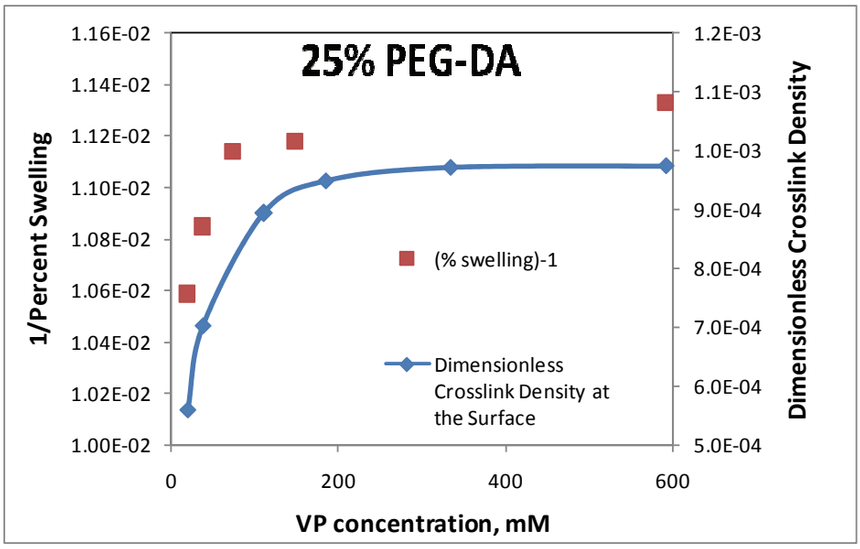

Fig. 4. Comparison of the dimensionless crosslink density of GLP-1 functionalized PEG hydrogel membrane and inverse of experimental swelling ratio versus VP concentration for 25% PEG-DA in prepolmer solution. ([TEA]=225 mM, [acrl-PEG-GLP-1=14. 8 μM, photopolymerization time=150 seconds) Squares denote experimental measurements and line represents model simulation.

Effects of VP and PEG-DA Concentrations on Crosslink Density. Crosslink density is an important property of PEG hydrogels, and is related to the permeability of the membrane. Membranes with higher the values of crosslink densities will be less permeable. The overall crosslink density (i. e. that for the membrane as a whole) was described earlier, and is defined as the ratio of QBP balance (F_1) to the first moment of dead polymer chains (Q_1), expressed as:(Kizilel, Perez-Luna and Teymour 2006)

$$\rho = \frac{[F_1]}{[Q_1]} \tag{33}$$

Highly crosslinked membranes (membranes with lower permeability and high mechanical strength) were obtained, as the concentration of VP in the precursor solution was increased. In our recent study for the modeling of biofunctional PEG hydrogel, propagation rate coefficient (k_{p11}) and termination rate coefficient (k_{tc11}), which were inversely proportional with the concentration of VP, were expressed as a function of VP concentration. The swelling measurements in that study also confirmed the positive effect of VP on crosslink density (Figure 4). The observed and predicted increases in crosslink density as a function of VP concentration was a direct result of increased acrylate conversion, as was observed by White et al. (White, Liechty and Guymon 2007). The increase of VP concentration influences crosslink density as a result of increase in the rate of polymerization. It has been shown in previous studies that significant differences in the polymerization rates would be observed with incorporation of VP, and that in VP/diacrylate polymerization systems adding VP increases polymerization rate. (White, Liechty and Guymon 2007) Furthermore, copolymerization of VP with acrylates can significantly increase the overall conversion of a crosslinked acrylate polymer, which can influence the crosslink density and thermomechanical properties. The results obtained in the recent study by Kızılel also emphasize that using optimal amounts of VP in the prepolymer solution allow significant increase in the crosslink density, and improvement in properties. Above a critical VP concentration (~185 mM), the influence of mono-vinyl monomer, VP, on hydrogel crosslink density was not observed; probably due to the maximum acrylate conversion achieved around 185 mM VP (Figure 5). The observed increases in crosslink densities were a direct result of increases in acrylate conversion, and above a critical concentration, the effect of VP, mono-vinyl monomer, on conversion was not sufficient to increase crosslink density further. The effect of VP concentration on crosslink density is illustrated in figure 5. As shown, the capsule crosslink density decreases with location for all the cases studied. This also shows that the capsule crosslink density decreases with membrane location moving from cell surface to membrane surface. The presence of gradient in crosslink density is a unique feature of this mathematical model and would be very difficult to obtain experimentally. Thus, this model could help design better transport properties and/or surface properties (polymer brush at the hydrogel-liquid interface) for these interfacially photopolymerized hydrogels. It was also observed that the crosslink densities will be higher for membranes obtained for higher PEG-DA concentration in the prepolymer. The lower crosslink densities obtained for the lower PEG-DA concentration (15 % (w/v)) was consistent with previous predictions of Kızılel et al. ,(Kizilel, Perez-Luna and Teymour 2006) and other studies, (Cruise, Hegre, Scharp and Hubbell 1998) and was explained by the presence of lower number of bi-functional monomers compared to the higher (25 and 40 % (w/v)) PEG-DA conditions. The fact that increasing PEG-DA concentrations decreased permeabilities of proteins implies that higher concentrations of PEG-DA in the prepolymer increases crosslink density, and that this result is consistent with the simulation results of this study. Lower concentration of bifunctional monomer results in a less branched and hence, less crosslinked structure. This result also emphasizes that, by increasing PEG-DA concentrations in the prepolymer solution, one would obtain membranes with higher crosslink densities and higher mechanical strength, which would mean lower membrane permeability.

Effects of VP and PEG-DA Concentrations on GLP-1 Incorporation. Incorporation of peptides to develop bioactive PEG hydrogels is an archetypal engineering problem, which requires the control of physical and chemical properties. In order to develop a functional extracellular matrix mimic, hydrogel crosslink density or mechanical properties,

incorporation of peptides, thickness of the membrane, and transport kinetics must be tuned effectively. (Griffith and Naughton 2002; Saha, Pollock, Schaffer and Healy 2007)

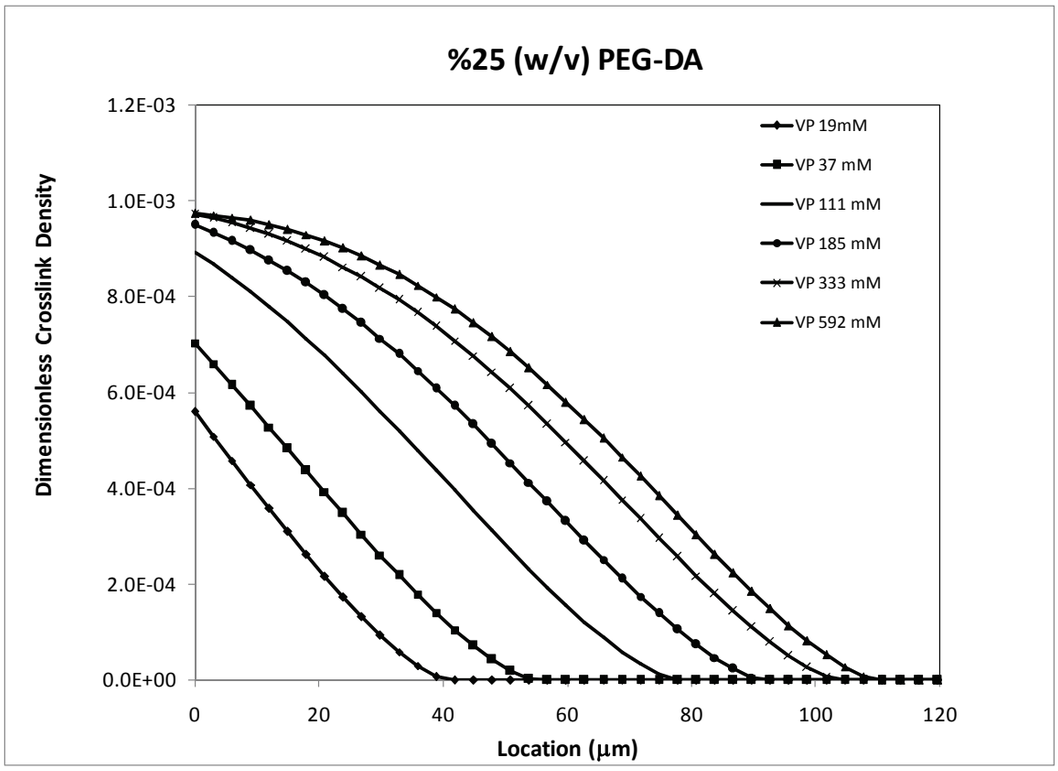

Fig. 5. Effect of concentration changes of VP on the dimensionless crosslink density versus location of GLP-1 functionalized PEG hydrogel membrane ([TEA]=225 mM, [acrl-PEG-GLP-1=14. 8 μM), 25% (w/v) PEG-DA in prepolmer solution.

GLP-1, a potent incretin hormone produced in the L cells of the distal ileum, stimulates insulin gene transcription, islet growth, and neogenesis. (MacDonald, El-kholy, Riedel, Salapatek, Light and MB 2002) Therefore, when GLP-1 is immobilized within the PEG hydrogel capsule around the islet, insulin secretion in response to high glucose levels was expected to increase, thereby reducing the number of islets required to normalize blood glucose of a diabetic patient, and improving the insulin secretion capability of microencapsulated islets. Recently, it was shown that, GLP-1 coated islets exhibited a higher response to glucose challenge, in terms of insulin secretion, compared to the untreated islets *in vitro*. (Kizilel, Scavone, Liu, Nothias, Ostrega, Witkowski and Millis 2010) This suggested that similar effect could be observed when GLP-1 is immobilized within the PEG hydrogel capsule around the islet. Therefore, it was important to design PEG hydrogel coatings with high GLP-1 concentrations at points closer to the surface in the case of islet microencapsulation within PEG hydrogel. This should allow interaction of GLP-1 with its receptor on insulin secreting β-cells, which will subsequently stimulate insulin secretion in response to high glucose. Therefore, the mathematical model developed, included acrl-PEG-GLP-1 as the third monomer of the polymerization process, due to the presence of acrylate group in the acrl-PEG-GLP-1 conjugate structure. As a result, the concentration of GLP-1 within the PEG hydrogels as a function of photopolymerization time or membrane location

for different PEG-DA or VP concentrations could be predicted. Figure 6 illustrates the variation of GLP-1 concentration with location at the photopolymerization time of 150 seconds for various VP and PEG-DA concentrations. As shown, GLP-1 concentration decreases with location for all the conditions studied, as a result of gradient in monomer conversion. For 25 % PEG-DA in the prepolymer, the profile extends to further points at higher VP concentrations due to the fact that higher thicknesses obtained at higher VP concentrations (Figure 6). The presence of gradient of GLP-1 is a unique feature of this mathematical model, and surface initiated polymerization, and would be very difficult to characterize experimentally. Incorporation of GLP-1 within a biofunctional PEG hydrogel could be done via radiolabeling experiments for the case of bulk polymerization, however for the case of surface initiated polymerization, characterization of GLP-1 concentration versus hydrogel location would be an experimental challenge. Therefore, theoretical prediction of peptide concentrations (GLP-1 in this case) within a biofunctional PEG hydrogel formed via surface initiated polymerization is clearly an advantage in this field. The presence of GLP-1 gradient would also allow efficient localization of the peptide to the islet surface, and hence may result in increased possibility of the peptide's interaction with its receptor to enhance insulin secretion.

7. Modeling of PEG hydrogel membrane based on numerical fractionation technique:

The mathematical models for PEG hydrogel membranes mentioned in the previous section was developed based on the method of moments along with the pseudo-kinetic rate constant approach. (Hamielec and MacGregor 1983; Kizilel, Perez-Luna and Teymour 2009) As presented, the method of moments reduced the number of equations to be solved, and zeroth and first moments of dead polymer chains were calculated in order to determine the crosslink density of the overall hydrogel. However, in nonlinear polymerizations systems where the polymer chain branching and/or crosslinking lead to the formation of a gel phase, the second and higher molecular weight moments diverge at the gel point. Thus a numerical solution past the gel point cannot be carried out into the post gel regime. In this study, in order to obtain a numerical solution past the gel point, we used the Numerical Fractionation (Teymour and Campbell 1994; Kizilel, Perez-Luna and Teymour 2009) (NF) technique, which refers to the numerical isolation of various polymer generations based on the degree of complexity of their microstructure. NF utilizes the kinetic approach but is based on a "variation" of the classical method of moments and is a powerful method to describe and model polymerization systems that result in gel formation. The technique has been used by various researchers to model different nonlinear polymerization systems. (Kizilel, Papavasiliou, Gossage and Teymour 2007; Arzamendi and Asua 1995; Kizilel 2004) The NF technique segregates the polymer into two distinct phases, a soluble (sol) phase and a gel phase. Modeling the sol phase and isolating the gel phase allows for the determination of the polymer properties such as, the gel point, and the reconstruction of the polymer molecular weight distribution (MWD). Isolation of the sol from the gel makes it possible to predict polymer properties in the post-gel region. Furthermore, the sol fraction is subdivided into generations that are composed of linear and branched polymer chains. The basic assumption of the NF technique is that gel is formed via a geometric growth mode present in the reacting system. Linear polymerization will not lead to gel formation. In order for gel formation to occur, a re-initiation reaction has to be coupled to a reaction in

which two radical chains join, such as termination by combination or having a radical react through a pendant double bond. The geometric growth mode applies specifically to the generations. Rules that govern the transfer from one generation to the next are as follows: Transfer to first generation occurs through a branching (e. g. chain transfer to polymer) or crosslinking reaction (reaction through a pendant double bond). The resulting polymer can keep adding linear polymer chains, but still belong to the first generation. Transfer to second generation will occur if two first generation molecules combine, e. g. through termination by the combination of two radicals or having a radical react through a pendant double bond. A polymer molecule belonging to the second generation can keep adding more linear or first generation branched polymer, but will only transfer to third generation when it combines with another second generation molecule. Combination of molecules belonging to different generations will result in the combined molecule belonging to the higher generation (Scheme 3).

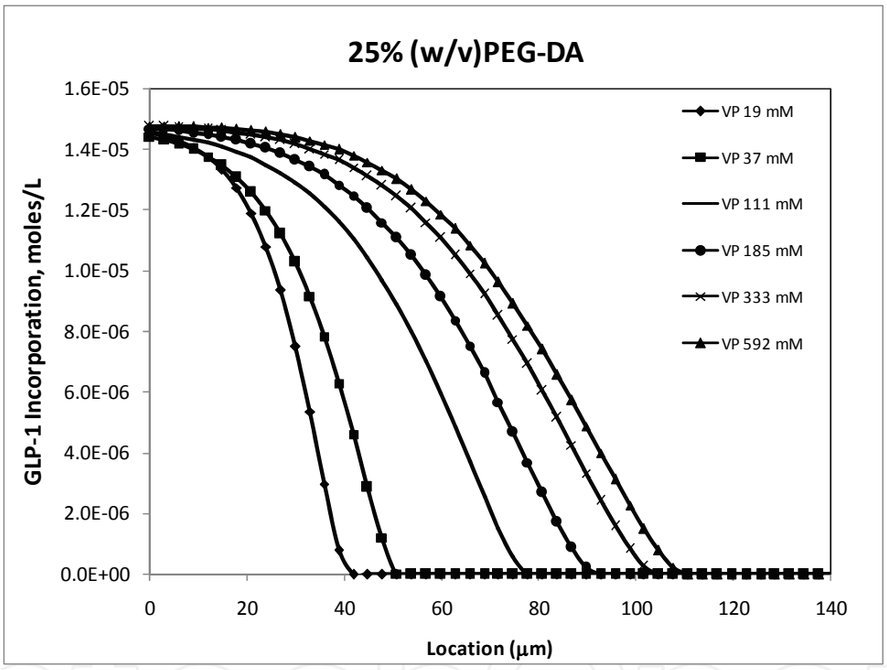

Figure 6. Effect of concentration changes of VP on the GLP-1 incorporation within the hydrogel versus location of GLP-1 functionalized PEG hydrogel membrane ([TEA]=225 mM, [acrl-PEG-GLP-1=14. 8 μM) 25% (w/v) PEG-DA in prepolmer solution.

The application of the NF technique for the process of PEG-DA hydrogel formation on substrate surfaces through interfacial photopolymerization was the first instance of the previous applications which involved homogeneously mixed systems with no spatial distribution. The application of this technique to dynamic membrane growth allowed the prediction of spatial profiles for the gel fraction, molecular weight properties, composition and crosslink density. Insight obtained from the model was also used to propose methodologies for the design of membranes with predetermined property profiles, such as progression through gelation, gelation time, crosslink density of the gel and soluble phases, degree of gel and sol fraction that might lead to advanced applications in biosensors and tissue engineering.

The authors used similar kinetic mechanism in the NF model, where they considered the polymerization system consisting of initiation, propagation, chain transfer to TEA, radical termination by combination and reaction through pendant double bond. (Kizilel, Perez-Luna and Teymour 2009) Chain transfer to PEG-DA (and hence to polymer) would provide an additional branching mechanism, which was not considered in the model development. It was also assumed that the terminal model of copolymerization was applicable and termination by disproportionation was not included. The copolymerization of *A (VP)* and *B (PEG-DA)* was considered, and the symbols A_{ijkl} or B_{ijkl} were used to indicate the type of monomer unit at the chain end identity of the propagating radical, where the four subscripts represented respectively the generation, the total chain length of each radical (live) and dead polymer, the number of unreacted pendant double bonds (PDB), and the number of quaternary branch points (QBP).

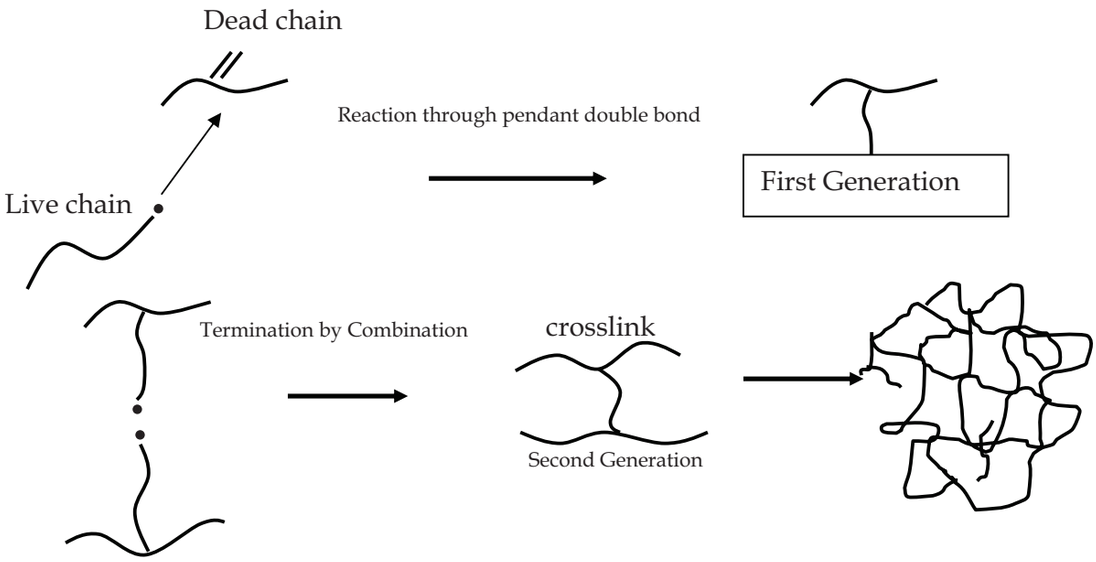

Scheme 3. Reactions leading to gel formation.

Initiation:

In this step the initiator radical (R_{in}), which is also called α-amino radical in this system, forms as a result of its reaction with eosin Y and reacts with the monomers to form live radicals of length one.

$$Y_{ac} \Leftrightarrow Y^* \qquad \nu K \tag{34}$$

$$Y^* + C_{TEA} \rightarrow Y_{in} + R_{in}\bullet \qquad k_f \tag{35}$$

$$R_{in}\bullet + A \rightarrow A_{0100}\bullet \qquad k_{i1} \tag{36}$$

$$R_{in}\bullet + B \rightarrow B_{0110}\bullet \qquad k_{i2} \tag{37}$$

where $\nu K = \nu \frac{k_1}{k_{-1}}$, K is the equilibrium constant for excitation and, νK represents the amount of excitation radiation absorbed by eosin Y molecules. Thus, ν would take into account the

intensity of the light source because an increase of excitation intensity would result in a larger number eosin molecules excited to the triplet state.

Propagation

Propagation of the two monomers, *A (VP)* and *B (PEG-DA)* leads to two types of propagating species, one with *A* at the propagating end and the other with *B.* These are represented by A• and *B*•. This classification is made because the reactivity of the propagating species is dependent on the monomer unit at the end of the chain. (Dotson, Galvan, Laurence and Tirrell 1996; Scott and Peppas 1999) Radical chains of length j react by adding monomer units to the polymer chain to form longer radical chains of length j+1 according to the following mechanism:

$$A_{ijkl}\bullet + A \rightarrow A_{i,j+1,k,l}\bullet \quad k_{p11} \tag{38}$$

$$A_{ijkl}\bullet + B \rightarrow B_{i,j+1,k+1,l}\bullet \quad k_{p12} \tag{39}$$

$$B_{ijkl}\bullet + A \rightarrow A_{i,j+1,k,l}\bullet \quad k_{p21} \tag{40}$$

$$B_{ijkl}\bullet + B \rightarrow B_{i,j+1,k+1,l}\bullet \quad k_{p22} \tag{41}$$

Termination:

Termination by combination reaction leads to the formation of longer dead polymer chains. Termination by combination reaction must be taken into account because it also leads to branching and gelation.

$$A_{ijkl}\bullet + A_{opqr}\bullet \rightarrow P_{i',j+p,k+q,l+r}\bullet \quad k_{tc11} \tag{42}$$

$$A_{ijkl}\bullet + B_{opqr}\bullet \rightarrow P_{i',j+p,k+q,l+r}\bullet \quad k_{tc12} \tag{43}$$

$$B_{ijkl}\bullet + B_{opqr}\bullet \rightarrow P_{i',j+p,k+q,l+r}\bullet \quad k_{tc22} \tag{44}$$

Chain Transfer to TEA

The radicals can also react with the chain transfer agent, TEA. In this case the growing radical is transferred to TEA, which hinders the growth of a polymer chain while at the same time generating a free radical capable of starting the growth of another polymer chain as follows:

$$A_{ijkl}\bullet + TEA \rightarrow P_{ijkl} + R_{in}\bullet \quad k_{tr1} \tag{45}$$

$$B_{ijkl}\bullet + TEA \rightarrow P_{ijkl} + R_{in}\bullet \quad k_{tr2} \tag{46}$$

Reaction through a Pendant Double Bond:

When a newly formed radical reacts through a pendant double bond, a quaternary branch point is created.

$$A_{ijkl}\bullet + P_{opqr} \rightarrow B_{i',j+p,k+q,l+r-1}\bullet \quad k^*_{p12} \tag{47}$$

$$B_{ijkl}\bullet + P_{opqr} \rightarrow B_{i',j+p,k+q,l+r-1}\bullet \quad k^*_{p22} \tag{48}$$

The mathematical model was developed by formulating population balances on each species in the system, which included: the live and dead polymer chains for the overall polymer, linear polymer chains and subsequent polymer generations. A set of moments was then applied to the above mentioned species. The quasi-steady state approximation was applied to all radical species. The pseudo-kinetic rate constant equations, moment equations, boundary conditions, and membrane thickness equations were similar to the model developed for biofunctional PEG hydrogel membrane, which was mentioned in the previous section. The moments were derived from the population balances using the NF technique. (Kizilel, Perez-Luna and Teymour 2009)

Crosslink Density and Crosslink Density Distribution

NF offers the unique capability of following the evolution of moment equations for each generation in both the pre-gel and post-gel regimes. The crosslink density of a polymer chain is defined as the fraction of units on that chain that contains quaternary branch points. In the systems that gel, the gel has a higher crosslink density than the sol. In the NF model, five types of crosslink densities were considered: the overall crosslink density (i. e., that for the polymer as whole), the crosslink density of each generation, the crosslink density of the sol, the crosslink density of the branched sol, and the crosslink density of the gel.

Figure 7 displays crosslink density versus time for each generation 1-10 (linear polymer has a crosslink density of zero and belongs to the zeroth generation), at the islet surface, for the surface initiated photopolymerization of PEG-DA. The geometric growth mechanism by which the generations were defined by the NF technique, explains the reason behind the collapse of the crosslink density curves for the higher generations onto a single curve. The collapse also demonstrates that in a polymerizing system, the intensive properties of the higher molecular weight molecules tend towards the same value.

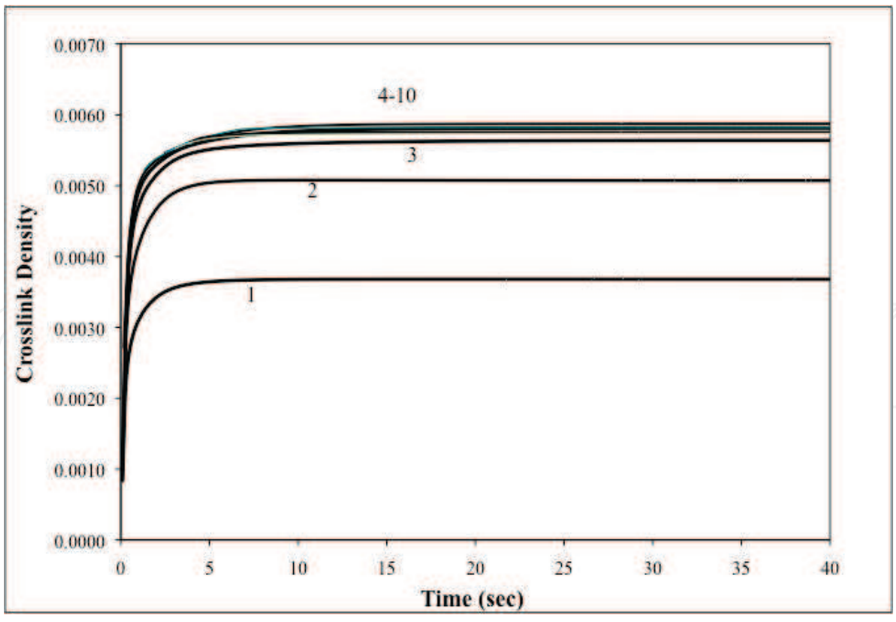

Fig. 7. Average crosslink density for each generation versus time at the cell surface (x=0 μm)

In addition to the crosslink density definitions given for each generation and for the overall polymer, NF technique was used to calculate crosslink densities for the sol (r_S), the branched sol (r_B), and the gel (r_G) which are defined by the following equations:

Crosslink density of the sol:

$$\rho_S = \frac{\sum_{i=1}^{n_C} F_{i,1}}{\sum_{i=1}^{n_C} Q_{i,1}} \tag{49}$$

Crosslink density of the branched sol:

$$\rho_B = \frac{\sum_{i=1}^{n_C} F_{i,1}}{\sum_{i=1}^{n_C} Q_{i,1}} \tag{50}$$

Crosslink density of the gel:

$$\rho_G = \frac{F_1 - \sum_{i=1}^{n_C} F_{i,1}}{Q_1 - \sum_{i=0}^{n_C} Q_{i,1}} \tag{51}$$

where, n_c is the highest generation modeled as sol. Figure 8 displays the crosslink densities of the sol, the branched sol, the gel, and overall polymer versus time for the process of hydrogel formation through surface initiated photopolymerization of PEG-DA at various membrane locations. As it is shown in the figure, crosslink densities of the sol (r_S) and the overall polymer (r) coincide up to the gel point. After the gel point, r continues to increase while r_S decreases due to the preferential loss of the larger sol molecules to the gel. The reason for the saturation behavior of the gel phase and stationary profile for the branched sol phase is due to the consumption of PEG-DA monomer. Initially PEG-DA concentration is equal to its bulk value at all points, however, once the membrane starts to grow away from the surface, PEG-DA (monomer B) cannot diffuse through the membrane, only VP can. So, the total number of unreacted pendant double bonds continually decreases and at this point only growth mechanism available is propagation with VP (monomer A). This explains the saturation of overall and gel crosslink density.

8. Other mathematical models developed for PEG hydrogel membranes

In the design of hydrogels for biomedical applications controlling the swelling ratio, diffusion rate, and mechanical properties of a crosslinked polymer is important, where each of these factors depends strongly on the degree of crosslinking. Primary cyclization occurs when a propagating radical reacts intramolecularly with a pendant double bond on the same chain, and decreases the crosslinking density which results in an increase in the molecular weight between crosslinks. The extent of primary cyclization is strongly affected by solvent concentration. Elliott *et al.* investigated the effect of solvent concentration and comonomer composition on primary cyclization using a novel kinetic model and experimental measurement of mechanical properties for crosslinked PEG hydrogels. (Elliott,

Anseth and Bowman 2001) The authors investigated two divinyl crosslinking agents, diethyleneglycol dimethacrylate (DEGDMA) and polyethyleneglycol 600 dimethacrylate (PEG(600)DMA), and each was copolymerized with hydroxyethyl methacrylate (HEMA) and octyl methacrylate (OcMA). The model was further used to predict the gel point conversion and swelling ratio of PAA hydrogels polymerized in the presence of varying amounts of water. Model results showed that increasing the solvent concentration during the polymerization increases the molecular weight between crosslinks by nearly a factor of three, and doubles the swelling ratio. Furthermore, experimental results provided quantitative agreement with model predictions. The model was developed and solved the differential kinetic equations accounting for the difference in reactivity of the pendant double bonds spatially and during the polymerization. In order to capture the local dynamics and reactivity of the pendant double bonds, monomeric and pendant double bonds were tracked separately. Based on the kinetic expression for a bimolecular collision, (the kinetic parameter k_p times the concentrations of monomeric double bonds and radical species in bulk solution [R_b]) the rate of consumption of monomeric double bonds was calculated. The bulk radicals [R_b] concentration was calculated using the pseudo-steady-state assumption. When a multifunctional monomer is consumed, a pendant double bond is created, which can react either by crosslinking or cyclization (Scheme 4).

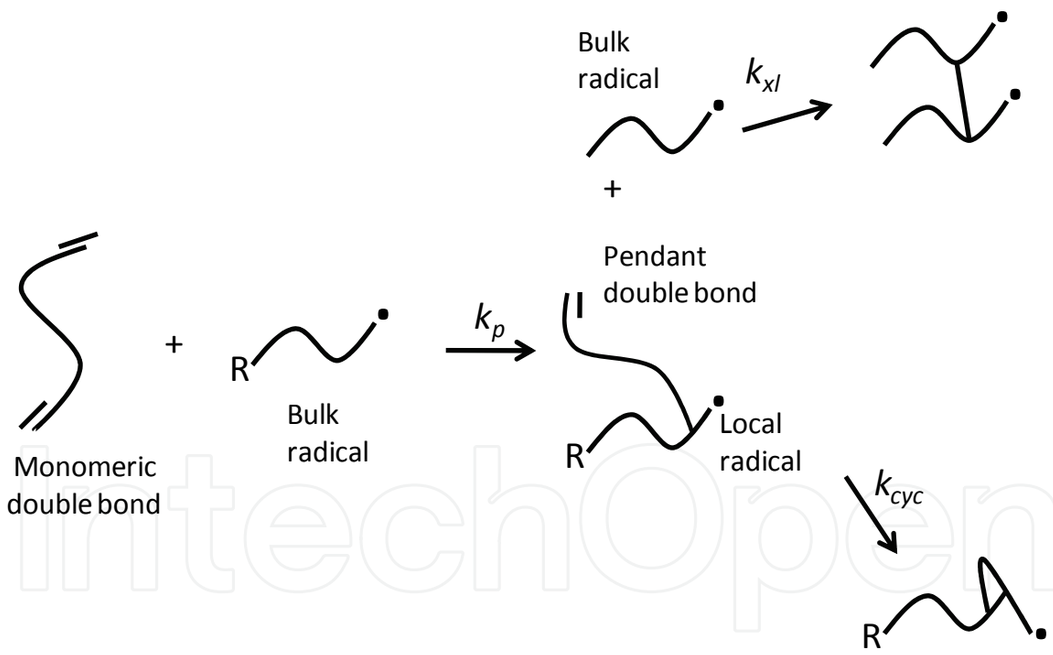

Scheme 4. Monomeric and pendant double bond reaction mechanism.

Both of these two mechanisms of propagation of pendant double bonds (R_{pen}) were considered in the model: the reaction of pendant double bonds with the radical on the same propagating chain (local radicals) to form cycles and the reaction of pendant double bonds with bulk radicals to form crosslinks. Secondary cycles were considered as equivalent to crosslinks. The difference in reactivity of the two competing mechanisms was also incorporated into the apparent radical concentrations relevant to the crosslinking and cyclization reactions.

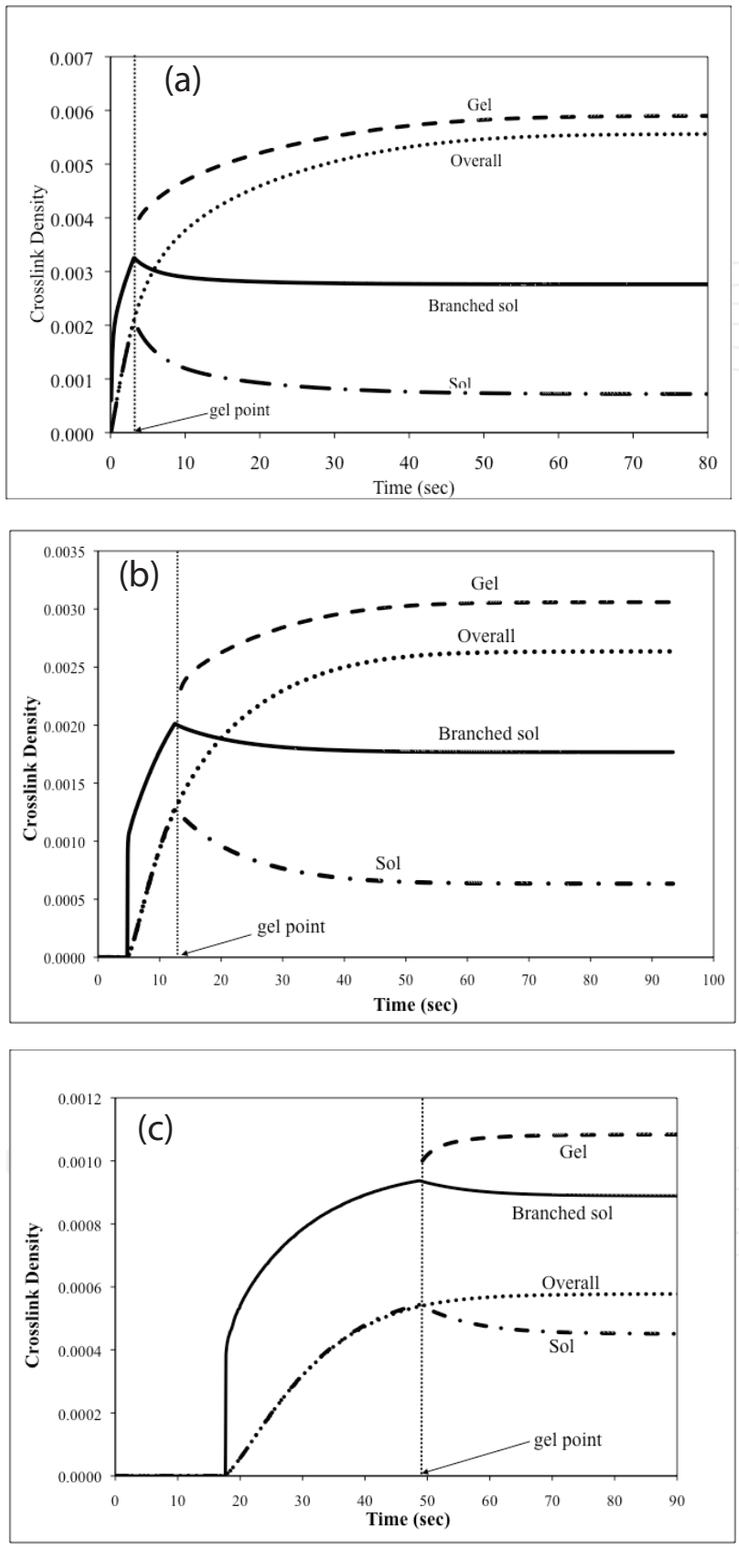

Fig. 8. Crosslink density for the sol, gel, branched sol, overall hydrogel versus time (a) at the cell surface (x=0 μm), (b) at x=56 μm, (c) at x=126 μm.

It is important to form degradable hydrogels having controlled network structure for applications related to both drug delivery and tissue engineering. Even though significant advances have occurred, these applications still cannot reach full potential without the availability of materials with tunable degradation behavior. To this end, Anseth and Bowman group developed thiol–acrylate degradable networks, which provided a simple method for forming degradable networks having specific degradation profiles. (Reddy, Anseth and Bowman 2005) These degradable thiol–acrylate networks were formed from copolymerizing a thiol monomer with PLA-b-PEG-b-PLA based diacrylate macromers (Scheme 5). The authors also developed a theoretical model to describe the kinetic chain length distribution, the bulk degradation behavior, and the reverse gelation point of these thiol–acrylate hydrogels.

Thiol–acrylate polymerizations are radical reactions that proceed through a unique mixed step-chain growth mechanism. In the first step, the thiyl radical propagates through the vinyl functional group to form a carbon based radical. In the second step of the reaction, this carbon-based radical either chain transfers to a thiol to regenerate a thiyl radical, or homopolymerizes in the third step with vinyl moieties. The basic reaction mechanism for the case of vinyl moieties that do not readily homopolymerize, as in pure thiol-ene reactions, is sequential propagation-chain transfer mechanism that leads to step growth polymerization. For most thiol-ene systems, the step growth mechanism dominates over the chain growth homopolymerization of the ene monomers. (Cramer and Bowman 2001) In thiol–acrylate systems on the other hand, where the acrylic vinyl monomer undergoes significant homopolymerization, a competition exists between step growth and chain growth mechanisms. Thus, in polymerization of thiol–acrylate systems, the reaction is a combination of both chain growth and step growth polymerization mechanisms. Therefore, the network structure and the degradation behavior is controlled by the balance of these two mechanisms.

$$\left.\begin{array}{r} RS\bullet + R'CH=CH_2 \xrightarrow{k_{pS-C}} R'C\bullet H-CH_2-SR \quad (52) \\ R'C\bullet H-CH_2-SR+RSH \xrightarrow{k_{CT}} R'CH_2-CH_2-SR+RS\bullet \quad (53) \end{array}\right\} \text{Step Growth}$$

$$R'C\bullet H-CH_2-SR+R'CH=CH_2 \xrightarrow{k_{pC-C}} \begin{array}{l} R'CH-CH_2-SR \\ \quad | \\ CH_2-C\bullet H-R' \end{array} \quad \text{Chain Growth} \quad (54)$$

In this recent study by Reddy et al, thiol functionality, as well as the relative stoichiometries of the thiol and acrylate functional groups were varied in order to control the kinetic chain length distribution and the concomitant degradation behavior of these systems. (Reddy, Anseth and Bowman 2005) The authors described theoretical bulk degradation profiles of degradable thiol–acrylate systems using modeling approaches where all the parameters were related to physically relevant aspects of the system. Since the degradation behavior was impacted by the number of crosslinks per kinetic chain,(Metters, Bowman and Anseth 2000) the kinetic chain length (KCL) distribution in these systems were first estimated. Then, the bulk degradation model based on probability and mean field kinetics were utilized to predict the degradation phenomena of the model thiol–acrylate degradable networks. It was shown that the KCL, and hence number of crosslinks per chain, were shown to decrease with increasing thiol concentration or decreasing thiol functionality, which could allow a

control on the network evolution and degradation behaviour. This approach is also applicable to other crosslinked, bulk degradable hydrogel networks that are formed through mixed step-chain polymerizations.

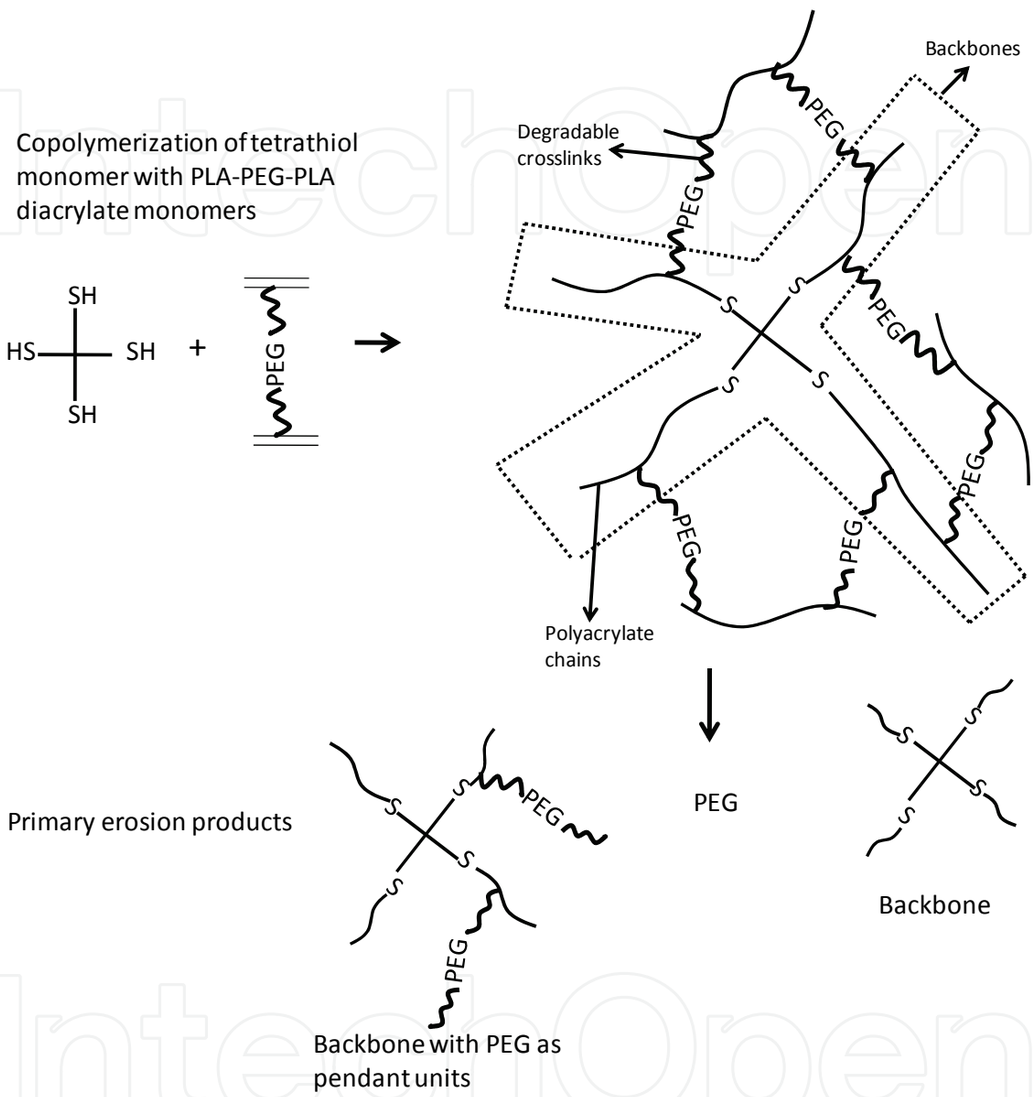

Scheme 5. Network formation of thiol–acrylate hydrogels and their subsequent degradation. The degradable polylactide units are represented as ~~~.

Despite the possibilities that exist for tuning the degradation of hydrolytically degradable gels, it is still impossible to predict exact degradation rate required for a specific cell source. Even though the degradation profile can be adjusted by addition of small amounts of macromonomers with longer or shorter PLA repeat units, the control that this allows over hydrogel degradation does not necessarily solve any problems associated with different rates of ECM production by different cell sources. One possible solution could be to replace PLA blocks with a block whose degradation depends on the concentration of a particular catalyst, then it might be possible to degrad the gel at a certain rate or not at all. This degradation could be tuned by the delivery of an enzyme released by the cells encapsulated

in the gel, which may correspond to the temporal development of ECM. In the study of Rice et al. hydrogels were synthesized by photopolymerization of a dimethacrylated tri-block copolymer, polycaprolactone-*b*-poly(ethylene glycol)-*b*-polycaprolactone (PEG-CAP-DM) macromonomers, where the crosslinks were degradable by a lipase enzyme. (Rice, Sanchez-Adams and Anseth 2006) The authors monitored the mass loss of these gels in the presence or absence of lipase, and compared this loss to the model predictions using a Michaelis-Menten derived kinetic model of reaction rate, coupled with a statistical aspect gleaned from structural information. It was observed that the rate of degradation, which was characterized by mass loss and mechanical testing, depended on both the number of repeat units in the cap blocks and also on the concentration of the active lipase enzyme. The model was developed to describe the mass loss in these materials, starting from reactions associated with classical enzyme kinetics and a simplified statistical adaptation of degradation in the gel network.

Besides, predicting the thickness and crosslink density of properties of PEG hydrogels for the purpose of immunoisolation barriers, the rational design of the hydrogel membranes require an understanding of protein diffusion and how alterations to the network structure affect protein diffusion. In order to address this need, Weber *et al.* studied the the diffusion of six model proteins with molecular weights ranging from 5700 to 67,000 g/mol through hydrogels of varying crosslinking densities, which were formed via the chain polymerization of dimethacrylated PEG macromers of varying molecular weight. (Weber, Lopez and Anseth 2009) Next, the diffusion coefficients for each protein/gel system that exhibited Fickian diffusion were estimated, using the release profiles of these proteins through these hydrogel membranes. Authors used the diffusion coefficients calculated using the Stokes-Einstein equation as a rough approximation for comparison with experimentally derived diffusion coefficients for proteins in hydrogels of varying crosslinking density. Insulin diffusivity was reduced by approximately 40% in the PEG gels with the lowest crosslinkable bond concentration and up to 60% in PEG gels with the highest concentration, when compared to the approximate diffusion coefficient in solution predicted by the Stokes–Einstein equation:

$$D_0 = \frac{kT}{6\pi\eta R_s} \tag{55}$$

The diffusion coefficients of larger proteins, such as trypsin inhibitor and carbonic anhydrase, on the other hand were decreased to approximately 10% of that in aqueous solution. The equation that correlates the diffusion coefficient of a given solute through a gel network (D_g) relative to that of the solute in solution (D_o) demonstrates that the diffusion is dependent on the solute radius (r_s) relative to a crosslinked network characteristic length (ζ) and the equilibrium water content of the hydrogel network, which is described as the polymer volume fraction in the gel (ν_2):

$$\frac{D_g}{D_o} = \left(1 - \frac{r_s}{\xi}\right)\exp\left(-Y\left(\frac{\nu_2}{1-\nu_2}\right)\right) \tag{56}$$

where Y is the ratio of the critical volume required for a successful translational movement of the solute to the average free volume per liquid molecule and it is usually taken as 1, and ν_2 is the inverse of the equilibrium swelling ratio (Q). The authors observed that the

diffusion coefficients were on the order of 10^{-6}–10^{-7} cm^2/s, such that protein diffusion time scales ($t_d=L^2/D$) from 0. 5-mm thick gels varied from 5 min to 24 h.

In this chapter, we introduced various approaches for modeling of PEG hydrogels for biomedical applications. The mathematical models developed for ECM-mimic of PEG hydrogels could be considered in the design of future PEG hydrogel or biofunctional PEG hydrogel systems where drugs, proteins or cells are microencapsulated within these membranes to predict the growth, crosslink density profiles, and the level of ligand incorporation. These models could also be utilized for the modulation of concentration of biological cues in highly permissive and biofunctional PEG hydrogels for optimizing engineered tissue formation.

9. References

Alcantar, N., E. Aydil & J. Israelachvili (2000) Polyethylene glycol-coated biocompatible surfaces. *J Biomed Mater Res,* 51, 343-351.

Amano, S. , N. Akutsu, Y. Matsunaga, K. Kadoya, T. Nishiyama, M. Champliaud & e. al. (2001) Importance of balance between extracellular matrix synthesis and degradation in basement membrane formation. *Exp Cell Res,* 271, 249-262.

Anseth, K. S. , C. M. Wang & C. N. Bowman (1994) Kinetic Evidence of Reaction-Diffusion during the Polymerization of Multi(Meth)Acrylate Monomers. *Macromolecules,* 27, 650-655.

Anseth, K. S. , C. M. Wang & C. N. Bowman (1994) Reaction Behavior and Kinetic Constants for Photopolymerizations of Multi(Meth)Acrylate Monomers. *Polymer,* 35, 3243-3250.

Arzamendi, G. & J. Asua (1995) Modeling Gelation and Sol Molecular Weight Distribution in Emulsion Polymerization. *Macromolecules,* 28, 7479-7490.

Aumaille, M. & N. Smyth (1998) The role of laminins in basement membrane function. *Anat*, 1-21.

Babensee, J. , L. McIntire & A. Mikos (2000) Growth factor delivery for tissue engineering. *Pharm Res,* 17, 497-504.

Badylak, S. (2002) The extracellular matrix as a scaffold for tissue reconstruction. *Semin Cell Dev Biol,* 13, 377-383.

Badylak, S. (2007) The extracellular matrix as a biological scaffold material. *Biomaterials,* 28, 3587-3593.

Bamford, C. & H. Tompa (1954) The Calculation of Molecular Weight Distributions From Kinetic Schemes. . *Trans. Faraday SOC,* 50, 1097.

Beamish, J. , J. Zhu, K. Kottke-Marchant & R. Marchant (2010) The effects of monoacrylate poly(ethylene glycol) on the properties of poly(ethylene glycol) diacrylate hydrogels used for tissue engineering. . *J Biomed Mater Res A,* 92, 441-450.

Beck, K. , I. Hunter & J. Engel (1990) Structure and function of laminin: anatomy of a multidomain glycoprotein. *FASEB*, 148-60.

Brodsky, B. & J. Ramshaw (1997) The collagen triple-helix structure. *Matrix Biol*, 545-54.

Bryant, S. , J. Arthur & K. Anseth (2005) Incorporation of tissue-specific molecules alters chondrocyte metabolism and gene expression in photocrosslinked hydrogels. *Acta Biomater* 1, 243-252.

Burdick, J. , M. Mason, A. Hinman, K. Thorne & K. Anseth (2002) Delivery of osteoinductive growth factors from degradable PEG hydrogels influences osteoblast differentiation and mineralization. . *J Control Release,* 83, 53-63.

Buxton, A. , J Zhu, R. Marchant, J. West, J. Yoo & B. Johnstone (2007) Design and characterization of poly(ethylene glycol) photopolymerizable semiinterpenetrating networks for chondrogenesis of human mesenchymal stem cells. *Tissue Eng,* 13, 2549-2560.

Cai, S. , Y. Liu, X. Zheng & G. Prestwich (2005) Injectable glycosaminoglyosaminoglycan hydrogels for controlled release of human basic fibroblast growth factor. *Biomaterials,* 26, 6054-6067.

Celse, K. , E. Poschl & T. Aigner (2003) Collagens-structure, function, and biosynthesis. *Adv Drug Deliv Rev*, 1513-46.

Chang, C. & Z. Werb (2001) The many faces of metalloproteases: cell growth, invasion, angiogenesis and metastasis. *Trends Cell Biol* 11, S37-S43.

Chen, W. , C. Chang & M. Gilson (2006) Concepts in receptor optimization: targeting the RGD peptide. *J Am Chem Soc* 128, 4675-4684.

Cheung, C. & K. A. KS (2006) Synthesis of immunoisolation barriers that provide localized immunosuppression for encapsulated pancreatic islets. *Bioconjug Chem,* 17, 1036-1042.

Cheung, C. , S. McCartney & K. A. KS (2008) Synthesis of polymerizable superoxide dismutase mimetics to reduce reactive oxygen species damage in transplanted biomedical devices. *Adv Funct Mater,* 18, 3119-3126.

Clapper, J. , J. Skeie, R. Mullins & C. Guymon (2007) Development and characterization of photopolymerizable biodegradable materials from PEG-PLA-PEG block macromonomers. . *Polymer* 48, 6554.

Cohen, M. , D. Joester, B. Geiger & L. Addadi (2004) Spatial and temporal sequence of events in cell adhesion: from molecular recognition to focal adhesion assembly. *ChemBioChem,* 5, 1393-1399.

Cramer, N. & C. Bowman (2001) Kinetics of thiol–ene and thiol–acrylate photopolymerizations with real-time fourier transform infrared. *Journal of Polymer Science Part A: Polymer Chemistry,* 39, 3311-3319.

Cramer, N. , S. Reddy, A. O'Brien & C. B. CN (2003) Thiol-ene photopolymerization mechanism and rate limiting step changes for various vinyl functional group chemistries. *Macromolecules,* 36, 7964-7969.

Cruise, G. M. , O. D. Hegre, D. S. Scharp & J. A. Hubbell (1998) A sensitivity study of the key parameters in the interfacial photopolymerization of poly(ethylene glycol) diacrylate upon porcine islets. *Biotechnology and Bioengineering,* 57, 655-665.

Cruise, G. M. , D. S. Scharp & J. A. Hubbell (1998) Characterization of permeability and network structure of interfacially photopolymerized poly(ethylene glycol) diacrylate hydrogels. *Biomaterials,* 19, 1287-1294.

Cukierman, E. , R. Pankov & K. Yamada (2002) Cell interactions with threedimensional matrices. *Curr Opin Cell Biol* 14, 633-639.

Cushing, M. & K. A. KS (2007) Hydrogel cell culture. *Science* 316, 1133-1134.

DeForest, C. , B. Polizzotti & K. A. KS (2009) Sequential click reactions for synthesizing and patterning three-dimensional cell microenvironments. *Nature Materials,* 8, 659-664.

Dotson, N. , R. Galvan, R. Laurence & M. Tirrell. 1996. *Polymerization Process Modeling*. New York: VCH Publishers.

Dudhia, J. (2005) Aggrecan, aging and assembly in articular cartilage. *Cell Mol Life Sci*, 2241-56.

Ehrbar, M. , S. Rizzi, R. Hlushchuk, V. Dionov, A. Zisch, J. Hubbell, F. Weber & M. Lutolf (2007) Enzymatic formation of modular cell-instructive fibrin analogs for tissue engineering. *Biomaterials,* 28, 3856-3866.

Ehrbar, M. , S. Rizzi, R. Schoenmakers, B. M. BS, J. H. JA, F. Weber & M. Lutolf (2007) Biomolecular hydrogels formed and degraded via site-specific enzymatic reactions. *Biomacromolecules,* 8, 3000-3007.

Elisseeff, J. , K. Anseth, D. Sims, W. McIntosh, M. Randolph & R. Langer (1999) Transdermal photopolymerization for minimally invasive implantation. *Proc Natl Acad Sci U S A,* 96, 3104-3107.

Elliott, J. , K. Anseth & C. Bowman (2001) Kinetic modeling of the effect of solvent concentration on primary cyclization during polymerization of multifunctional monomers *Chem Eng Sci,* 56, 3173-3184.

Ellis, V. & G. Murphy (2001) Cellular strategies for proteolytic targeting during migration and invasion. *FEBS Lett,* 506, 1-5.

Feldstein, M. , V. Igonin, T. Grokhovskaya, T. Lebedeva, S. Kotomin, V. Kulichikhin, N. Plate, K. Brain, V. James & K. Walters (1997) Performance of hydrophilic transdermals as an explicit function of the molecular structure of polymer matrix. *Perspectives of Percutaneous Penetration,* 5b, 228-232.

Feldstein, M. , N. Plate, T. Sohn, V. Voicu & N. R. C. c. a. f. p. f. protection (1999) A structure-property relationship and quantitative approach to the development of universal transdermal drug delivery system. *NBC Risks - Current capabilities and future perspectives for protection*, 441-58.

Feldstein, M. , V. Tohmakhchi, L. Malkhazov, A. Vasiliev & N. Plate (1996) Hydrophilic polymeric matrices for enhanced transdermal drug delivery. *Int J Pharm,* 2, 229-42.

Fisher, J. , D. Dean, P. Engel & A. Mikos (2001) Photoinitiated polymerization of biomaterials. *Annu Rev Mater Res,* 31, 171-181.

Fosang, A. , K. Last, V. Knauper, G. Murphy & P. Neame (1996) Degradation of cartilage aggrecan by collagenase-3 (MMP-13). *FEBS Lett,* 380, 17-20.

Gailit, J. & R. Clark (1994) Wound repair in the context of extracellular matrix. *Curr Opin Cell Biol* 717-25.

Giannelli, G. , J. Falk-Marzillier, O. Schiraldi, W. Stetler-Stevenson & V. Quaranta (1997) Induction of cell migration by matrix metalloprotease-2 cleavage of laminin-
5. *Science* 277, 225-228.

Girotti, A. , J. Reguera & J. Rodriguez-Cabello (2004) Design and bioproduction of recombinant multi(bio)functional elastin-like protein polymer containing cell adhesion sequences for tissue engineering purposes. *J Mater Sci Mater Med* 15, 479-484.

Gobin, A. & J. West (2003) Effects of epidermal growth factor on fibroblast migration through biomimetic hydrogels. *Biotechnol Prog* 19, 1781-1785.

Gole, T. & U. Pohl (2002) Laminin binding conveys mechanosensing in endothelial cells. *News Physiol Sci*, 166-9.

Griffith, L. G. & G. Naughton (2002) Tissue engineering - Current challenges and expanding opportunities. *Science,* 295, 1009-+.

Guidetti, G. , B. Bartolini, B. Bernardi, M. Tira, M. Berndt, C. Balduini & e. al. (2004) Binding of von Willebrand factor to the small proteoglycan decorin. *FEBS Lett,* 574, 95-100.

Haas, T. & E. Plow (1994) Integrin-ligand interactions: a year in review. *Curr Opin Cell Biol,* 6, 656-662.

Hahn, M. , M. McHale, E. Wang, R. Schmedlen & J. West (2007) Physiologic pulsatile flow bioreactor conditioning of poly(ethylene glycol)-based tissue engineered vascular grafts. . *Ann Biomed Eng,* 35, 190-200.

Halstenberg, S. , A. Panitch, S. Rizzi, H. Hall & J. Hubbell (2002) Biologically engineering protein-graft-poly(ethylene glycol) hydrogels: a cell adhesive and plasmindegradable biosynthetic material for tissue repair. *Biomacromolecules,* 3, 710-723.

Hamielec, A. & J. MacGregor. 1983. *Polymer Reaction Engineering*. New York: Hanser Publisher.

Haubner, R. , R. Gratias, B. Diefenbach, S. Goodman, A. Jonczyk & H. Kessler (1996) Structural and functional aspects of RGD-containing cyclic pentapeptides as highly potent and selective integrin avb3 antagonists. *J Am Chem Soc,* 118, 7461-7472.

Haubner, R. , W. Schmitt, G. Holzemann, S. Goodman, A. Jonczyk & H. Kessler (1996) Cyclic RGD peptides containing b-turn mimetics. *J Am Chem Soc,* 118, 7881-7891.

Heino, J. (2007) The collagen family members as cell adhesion proteins. *BioEssays,* 29, 1001-1010.

Henricks, P. & F. Nijkamp (1998) Pharmacological modulation of cell adhesion molecules. *Eur J Pharmacol* 344.

Hern, D. & J. Hubbell (1998) Incorporation of adhesion peptides into nonadhesive hydrogels useful for tissue resurfacing. *J Biomed Mater Res* 39, 266-276.

Hersel, U. , C. Dahmen & H. Kessler (2003) RGD modified polymers: biomaterials for stimulated cell adhesion and beyond. *Biomaterials,* 24, 4385-4415.

Heuts, J. P. A. , R. G. Gilbert & L. Radom (1995) A priori prediction of propagation rate coefficients in free-radical polymerizations: Propagation of ethylene. *Macromolecules,* 28, 8771-8781.

Hoffman, A. (2002) Hydrogels for biomedical applications. *Adv Drug Delivery Rev,* 43, 3-12.

Horkay, F. , P. Basser, A. Hecht, E. Geissler & 2008; 128:135103. (2008) Gel-like behavior in aggrecan assemblies. *Chem Phys*, 135103.

Houllier, L. & B. Bunel (2001) Photoinitiated cross-linking of a thiol-methacrylate system. *Polymer,* 42, 2727-2736.

Hu, B. , J. Su & P. Messersmith (2009) Hydrogels cross-linked by native chemical ligation. *Biomacromolecules,* 10, 2194-2200.

Hubbell, J. (1998) Synthetic biodegradable polymers for tissue engineering and drug delivery. *Curr Opin Solid ST M,* 3, 246-251.

Hudalla, G. , T. Eng & W. Murphy (2008) An approach to modulate degradation and mesenchymal stem cell behavior in poly(ethylene glycol) networks. *Biomacromolecules,* 9, 842-849.

Humphries, M. & P. Newham (1998) The structure of cell-adhesion molecules. *Trends Cell Biol* 8, 78-83.

Huttenlocher, A. , R. Sandborg & A. Horwitz (1995) Adhesion in cell migration. *Curr Opin Cell Biol* 7, 697-706.

Hynd, M. , J. Frampton, N. Dowell-Mesfin, J. Turner & W. Shain (2007) Directed cell growth on protein-functionalized hydrogel surfaces. *J Neurosci Methods,* 162, 255-263.

Ifkovits, J. & J. Burdick (2007) Review: photopolymerizable and degradable biomaterials for tissue engineering applications. *Tissue Eng,* 13, 2369-2385.

Jensen, L. & N. Host (1997) Collagen: scaffold for repair or execution. *Cardiovasc Res,* 33, 535-539.

Ji, J. , R. F. Childs & M. Mehta (2001) Mathematical model for encapsulation by interfacial polymerization. *Journal of Membrane Science,* 192, 55-70.

Jiang, Z. , J. Hao, Y. You, Y. Liu, Z. Wang & X. Deng (2008) Biodegradable and thermosensitive hydrogels of poly(ethylene glycol)-poly(e-caprolactone-co-glycolide)-poly(ethylene glycol) aqueous solutions. . *J Biomed Mater Res A,* 87, 45-51.

Jo, Y. , J. Gantz, J. Hubbell & M. L. MP (2009) Tailoring hydrogel degradation and drug release via neighboring amino acid controlled ester hydrolysis. *Soft Matter,* 5, 440-446.

Johansson, S. , G. Svineng, K. Wennerberg, A. Armulik & L. Lohikangas (1997) Fibronectine-integrin interactions. *Front Biosci*, 126-146.

Katz, B. , E. Zamir, A. Bershadsky, Z. Kam, K. Yamada & B. Geiger (2000) Physical state of the extracellular matrix regulates the structure and molecular composition of cell-matrix adhesions. *Mol Biol Cell,* 11, 1047-1060.

Kaufmann, D. , A. Fiedler, A. Junger, J. Auernheimer, H. Kessler & R. Weberskirch (2008) Chemical conjugation of liner and cyclic RGD moieties to a recombinant elastin-mimetic polypeptide e a versatile approach towards bioactive protein hydrogels. *Macromol Biosci,* 8, 577-588.

Khetan, S. , J. Katz & J. Burdick (2009) Sequential crosslinking to control cellular spreading in 3-dimensional hydrogels. *Soft Mater,* 5, 1601-1606.

Kizilel, S. 2004. Theoretical and Experimental Investigation for Interfacial Photopolymerization of Poly(ethylene glycol) Diacrylate. In *Biomedical Engineering*. Chicago: Illinois Institute of Technology.

Kizilel, S. (2010) Mathematical Model for Microencapsulation of Pancreatic Islets within Biofunctional PEG Hydrogel. *Macromolecular Theory and Simulations,* DOI: ((mats. 201000033)).

Kizilel, S. , G. Papavasiliou, J. Gossage & F. Teymour (2007) Mathematical model for vinyl-divinyl polymerization. *Macromolecular Reaction Engineering,* 1, 587-603.

Kizilel, S. , V. H. Perez-Luna & F. Teymour (2004) Photopolymerization of poly(ethylene glycol) diacrylate on eosin-functionalized surfaces. *Langmuir,* 20, 8652-8658.

Kizilel, S. , V. H. Perez-Luna & F. Teymour (2006) Mathematical model for surface-initiated photopolymerization of poly(ethylene glycol) diacrylate. *Macromolecular Theory and Simulations,* 15, 686-700.

Kizilel, S. , V. H. Perez-Luna & F. Teymour (2009) Modeling of PEG Hydrogel Membranes for Biomedical Applications. *Macromolecular Reaction Engineering,* 3, 271-287.

Kizilel, S. , E. Sawardecker, F. Teymour & V. H. Perez-Luna (2006) Sequential formation of covalently bonded hydrogel multilayers through surface initiated photopolymerization. *Biomaterials,* 27, 1209-1215.

Kizilel, S. , A. Scavone, X. A. Liu, J. M. Nothias, D. Ostrega, P. Witkowski & M. Millis (2010) Encapsulation of Pancreatic Islets Within Nano-Thin Functional Polyethylene Glycol Coatings for Enhanced Insulin Secretion. *Tissue Engineering Part A,* 16, 2217-2228.

Kretlow, J. , L. Klouda & A. Mikos (2007) Injectable matrices and scaffolds for drug delivery in tissue engineering. *Adv Drug Deliv Rev* 59, 263-273.

Ksihara, S. , S. Matsumura & J. Fisher (2008) Synthesis and characterization of cyclic acetal based degradable hydrogels. *Eur J Pharm Biopharm,* 68, 67-73.

Kuhn, K. (1985) Structure and biochemistry of collagen. Aesthetic Plast Surg. 141-4.

Kuhn, K. (1994) Basement membrane (type IV) collagen. *Matrix Biol*, 439-45.

Kumagai, C. , M. Okano & Y. Kitagawa (2000) Three heterotrimeric laminins produced by human keratinocytes. *Cytotechnology*, 167-74.

Kumar, G. S. & D. C. Neckers (1991) Laser-Induced 3-Dimensional Photopolymerization Using Visible Initiators and Uv Cross-Linking by Photosensitive Comonomers. *Macromolecules,* 24, 4322-4327.

Leahy, D. , I. Aukhil & H. Erickson (1996) 2. 0Å crystal structure of a four-domain segment of human fibronectin encompassing the RGD loop and synergy region. *Cell Transplantation,* 84, 155-164.

Lee, J. , H. Lee & J. Andrade (1995) Blood compatibility of polyethylene oxide surfaces. *Prog Polym Sci* 20, 1043-1079.

Lee, K. & D. Mooney (2001) Hydrogels for tissue engineering. *Chem Rev,* 101, 1869-1879.

Lee, S. , J. Moon, J. Miller & J. West (2007) Poly(ethylene glycol) hydrogels conjugated with a collagenase-sensitive fluorogenic substrate to visualized collagenase activity during three-dimensional cell migration. *Biomaterials,* 28, 3163-3170.

Li, Q. , C. Williams, D. Sun, J. Wang, K. Leong & J. Elisseeff (2004) Photocrosslinkable polysaccharides based on chondroitin sulfate. *J Biomed Mater Res A,* 68, 28-33.

Liao, S. , C. Chan & S. Ramakrishna (2008) Stem cells and biomimetic materials strategies for tissue engineering. *Mater Sci Eng C,* 28, 1189-1202.

Lin, C. & K. Anseth (2009) Controlling affinity binding with peptide-functionalized poly(ethylene glycol) hydrogels. *Adv Funct Mater,* 19, 2325-2331.

Lin, X. , K. Takahashi, Y. Liu & P. Zamora (2006) Enhancement of cell attachment and tissue integration by a IKVAV containing multi-domain peptide. *BBA-Gen Subjects,* 1760, 1403-1410.

Locardi, E. , D. Mullen, R. Mattern & M. Goodman (1999) Conformations and pharmacophores of cyclic RGD containing peptides which selectively bind integrin avb3. *J Pept Sci,* 5, 491-506.

Luo, W. , C. Guo, J. Zheng, T. Chen, P. Wang & B. Vertel (2000) Aggrecan from start to finish. *Bone Miner Metab*, 51-6.

Lutolf, M. (2009) Spotlight on hydrogels. *Nat Mater* 8, 451-453.

Lutolf, M. & J. Hubbell (2005) Synthetic biomaterials as instructive extracellular microenvironments for morphogenesis in tissue engineering. *Nat Biotechnol,* 23, 47-55.

Luzak, B. , J. Golanski, M. Rozalski, M. Boncler & C. Watala (2003) Inhibition of collageninduced platelet reactivity by DGEA peptide. *Acta Biochim Pol,* 50, 1119-1128.

Ma, P. (2008) Biomimetic materials for tissue engineering. *Adv Drug Deliv Rev,* 60, 184-198.

MacDonald, P. , W. El-kholy, M. Riedel, A. Salapatek, P. Light & W. MB (2002) The multiple actions of GLP-1 on the process of glucose-stimulated insulin secretion. . *Diabetes* 51, S434-S442.

Malkoch, M. , R. Vestberg, N. Gupta, L. Mespouille, P. Dubois, A. Mason, J. Hedrick, Q. Liao, C. Frank, K. Kingsbury & C. Hawker (2006) Synthesis of well-defined hydrogel networks using Click chemistry. *Chem Commun*, 2774-2776.

Massia, S. & J. Hubbell (1992) Tissue engineering in the vascular graft. *Cytotechnology,* 10, 189-204.

Masters, K. , D. Shah, G. Walker, L. Leinwand & K. Anseth (2004) Designing scaffolds for valvular interstitial cells: cell adhesion and function on naturally derived materials. *J Biomed Mater Res A,* 71, 172-180.

Mel, A. d. , G. Jell, M. Stevens & A. Sefalian (2008) Biofunctionalization of biomaterials for accelerated in situ endothelialization: a review. *Biomacromolecules,* 9, 2969-2979.

Metters, A. , C. Bowman & K. Anseth (2000) A Statistical Kinetic Model for the Bulk Degradation of PLA-b-PEG-b-PLA Hydrogel Networks. *The Journal of Physical Chemistry B,* 104, 7043-7049.

Metters, A. & J. Hubbell (2005) Network formation and degradation behavior of hydrogels formed by Michael-type addition reactions. . *Biomacromolecules,* 6, 290-301.

Mineur, P. , A. Guignandon, C. Lambert, C. Lapiere & B. Nusgens (2005) RGDS and DGEA-induced [Ca2þ]i signaling in human dermal fibroblast. *BBA-Mol Cell Res,* 1746, 28-37.

Moon, J. , S. Lee & J. West (2007) Synthetic biomimetic hydrogels incorporated with Ephrin-A1 for therapeutic angiogenesis. *Biomacromolecules,* 8, 42-49.

Murphy, G. & J. Gavrilovic (1999) Proteolysis and cell migration: creating a path? *J. Curr Opin Cell Biol* 11, 614-621.

Murphy, G. , V. Knauper, S. Atkinson, J. Gavriliovic & D. Edwards (2000) Cellular mechanisms for focal proteolysis and the regulation of the microenvironment. *Fibrinol Proteol,* 14, 165-174.

Mydel, P. , J. Shipley, T. Adair-Kirk, D. Kelley, T. Broekelmann & R. Mecham (2008) Neutrophil elastase cleaves laminin-332 (lamini-5) generating peptides that are chemotactic for neutrophils. *J Biol Chem,* 15, 9513-9522.

Nagase, H. & G. Fields (1996) Human matrix metalloproteinase specificity studies using collagen sequence-based synthetic peptides. *Biopolymers,* 40, 399-416.

Neckers, D. C. , S. Hassoon & E. Klimtchuk (1996) Photochemistry and photophysics of hydroxyfluorones and xanthenes. *Journal of Photochemistry and Photobiology a-Chemistry,* 95, 33-39.

Nie, T. , R. Akins & K. Kiick (2009) Production of heparin-containing hydrogels for modulating cell responses. *Acta Biomater,* 5, 865-875.

Nomizu, M. , B. Weeks, C. Weston, W. Kim, H. Kleinman & Y. Yamada (1995) Structure-activity study of a laminin a1 chain active peptide segment IleeLyseValeAlaeVal (IKVAV). *FEBS Lett,* 365, 227-231.

Nuttelman, C. , M. Rice, A. Rydholm, C. Salinas, D. Shah & K. Anseth (2008) Macromolecular monomers for the synthesis of hydrogel niches and their application in cell encapsulation and tissue engineering. *Prog Polym Sci,* 33, 167-170.

Nuttelman, C. , M. Tripodi & K. Anseth (2005) Synthetic hydrogel niches that promote hMSC viability. . *Matrix Biol* 24, 208-218.

Obrink, B. , T. Laurent & B. Carlsson (1975) The binding of chondroitin sulphate to collagen. *FEBS Lett* 56, 166-169.

Odian, G. 2004. *Principles of Polymerization*. New Jersey: John Wiley and Sons, Inc.

Ogura, Y. , Y. Matsunaga, T. Nishiyama & S. Amano (2008) Plasmin induces degradation and dysfunction of laminin 332 (laminin 5) and impaired assembly of basement membrane at the dermal-epidermal junction. *Br J Dermatol,* 159, 49-60.

Ottani, V. , M. Raspanti & A. Ruggeri (2001) Collagen structure and functional implications. *Microscopy*, 251-60.

Papagiannopoulos, A. , T. Waign & T. Hardingham (2008) The viscoelasticity of self-assembled proteoglycan combs. *Faraday Discuss*, 337-57.

Park, Y. , M. Lutolf, J. Hubbell, E. Hunziker & M. W. M (2004) Bovine primary chondrocyte culture in synthetic matrix metalloproteinase-sensitive poly(ethylene glycol)-based hydrogels as a scaffold for cartilage repair. . *Tissue Eng,* 10, 515-522.

Patel, P. , A. Gobin, J. West & C. Patrick (2005) Poly(ethylene glycol) hydrogels system supports preadipocyte viability, adhesion, and proliferation. *Tissue Eng,* 11, 1498-1505.

Pathak, C. P. , A. S. Sawhney & J. A. Hubbell (1992) Rapid Photopolymerization of Immunoprotective Gels in Contact with Cells and Tissue. *Journal of the American Chemical Society,* 114, 8311-8312.

Peppas, N. , K. Keys, M. Torres-Lugo & A. Lowman (1999) Poly(ethylene glycol)-containing hydrogels in drug delivery. . *J Control Release,* 62, 81-87.

Pocza, P. , H. Suli-Vargham, Z. Darvas & A. Falus (2008) Locally generated VGVAPG and VAPG elastin-derived peptides amplify melanoma invasion via the galectin-3 receptor. *Int J Cancer,* 122, 1972-1980.

Polizzotti, B. , B. Fairbanks & K. Anseth (2008) Three-dimensional biochemical patterning of Click-based composite hydrogels via thiol-ene photopolymerization. *Biomacromolecules,* 9, 1084-1087.

Potts, J. & I. Campbell (1994) Fibronectin structure and assembly. *Curr Opin Cell Biol*, 648-55.

Reddy, S. , K. Anseth & C. Bowman (2005) Modeling of network degradation in mixed step-chain growth polymerizations. *Polymer,* 46, 4212-4222.

Reddy, S. , N. Cramer & C. Bowman (2006) Thiol-vinyl mechanisms. 1. Termination and propagation kinetics in thiol-ene photopolymerizations. *Macromolecules,* 39, 3673-3680.

Rhodes, J. & M. Simons (2007) The extracellular matrix and blood vessel formation; not just a scaffold. *J Cell Mol Med,* 11, 176-205.

Rhodes, J. & M. Simons (2007) The extracellular matrix and blood vessel formation; not just a scaffold. *Cell Mol Med*, 176-205.

Rice, M. , J. Sanchez-Adams & K. Anseth (2006) Exogenously Triggered, Enzymatic Degradation of Photopolymerized Hydrogels with Polycaprolactone Subunits: Experimental Observation and Modeling of Mass Loss Behavior. *Biomacromolecules* 7, 1968-1975.

Ruoslahti, E. (2003) The RGD story: a personal account. *Matrix Biol,* 22, 459-465.

Ruoslahti, E. & M. Pierschbacher (1987) New perspectives in cell adhesion: RGD and integrins. *Science,* 238, 491-497.

Rydholm, A. , K. Anseth & C. Bowman (2007) Effects of neighboring sulfides and pH on ester hydrolysis in thiol-acrylate photopolymers. *Acta Biomater,* 3, 449-455.

Rydholm, A., C. Bowman & K. Anseth (2005) Degradable thiol-acrylate photopolymers:polymerization and degradation behavior of an in situ forming biomaterial. . *Biomaterials,* 26, 4495-4506.

S'Engel, P. J. & A. Mikos (2000) Synthesis of poly(ethylene glycol)-tethered poly (propylene fumarate) and its modification with GRGD peptide. . *Polymer,* 41, 7595-7604.

Saha, K. , J. F. Pollock, D. V. Schaffer & K. E. Healy (2007) Designing synthetic materials to control stem cell phenotype. *Current Opinion in Chemical Biology,* 11, 381-387.

Salinas, C. & K. Anseth (2008) Mixed mode thiol-acrylate photopolymerizations for the synthesis of PEG-peptide hydrogels. *Macromolecules,* 41, 6019-6026.

Salinas, C. & K. A. KS (2008) The enhancement of chondrogenic differentiation of human mesenchymal stem cells by enzymatically regulated RGD functionalities. *Biomaterials,* 29, 2370-2377.

Sanborn, T. , P. Messersmith & A. Barron (2002) In situ crosslinking of a biomimetic peptide-PEG hydrogel via thermally triggered activation of factor XIII. *Biomaterials,* 23, 2703-2710.

Sands, R. & D. Mooney (2007) Polymers to direct cell fate by controlling the microenvironment. *Curr Opin Biotechnol* 18, 448-453.

Sawhney, A., C. Pathak & J. Hubbell (1993) Bioerodible hydrogels based on photopolymerized poly(ethylene glycol)-co-poly(a-hydroxy acid) diacrylate macromers. *Macromolecules* 26, 581-587.

Scott, J. (1995) Extracellular matrix, supramolecular organization and shape. *Anat*, 259-69.

Scott, R. & N. Peppas (1999) Kinetics of Copolymerization of PEG-Containing Multiacrylates with Acrylic Acid. *Macromolecules,* 32, 6149-6158.

Seiki, M. (2002) The cell surface: the stage for matrix metalloproteinase regulation of migration. *Curr Opin Cell Biol* 14:, 624-632.

Shin, H. , S. Jo & A. Mikos (2003) Biomimetic materials for tissue engineering. *Biomaterials,* 24, 4353-4364.

Silva, A. , C. Richard, M. Bessodes, D. Scherman & O. Merten (2009) Growth factor delivery approaches in hydrogels. *Biomacromolecules,* 10, 9-18.

Stach, M. , I. Lacik, D. Chorvat, M. Buback, P. Hesse, R. A. Hutchinson & L. Tang (2008) Propagation rate coefficient for radical polymerization of N-vinyl pyrrolidone in aqueous solution obtained by PLP-SEC. *Macromolecules,* 41, 5174-5185.

Teymour, F. & J. D. Campbell (1994) Analysis of the Dynamics of Gelation in Polymerization Reactors Using the Numerical Fractionation Technique. *Macromolecules,* 27, 2460-2469.

Tibbitt, M. & K. Anseth (2009) Hydrogels as extracellular matrix mimics for 3D cell culture. *Biotechnol Bioeng,* 103, 655-663.

Traub, W. (1978) Molecular assembly in collagen. *FEBS Lett,* 92, 114-120.

Truong, K. & J. West (2002) Photopolymerizable hydrogels for tissue engineering applications. *Biomaterials,* 23, 4307-4314.

Turk, B. , L. Huang, E. Piro & L. Cantley (2001) Determination of protease cleavage site motifs using mixture-based oriented peptide libraries. *Nat Biotechnol,* 19, 661-667.

Valdes-aguilera, O., C. P. Pathak, J. Shi, D. Watson & D. C. Neckers (1992) Photopolymerization Studies Using Visible-Light Photoinitiators. *Macromolecules,* 25, 541-547.

Vertel, B. (1995) The ins and outs of aggrecan. *Trends Cell Biol*, 458-64.

Webb, D. , J. Parsons & A. Horwitz (2002) Adhesion assembly, disassembly and turnover in migrating cells e over and over and over again. *Nat Cell Biol,* 4, E97-E99.

Weber, L. M. & K. S. Anseth (2008) Hydrogel encapsulation environments functionalized with extracellular matrix interactions increase islet insulin secretion. *Matrix Biology,* 27, 667-673.

Weber, L. M. , K. N. Hayda & K. S. Anseth (2008) Cell-Matrix Interactions Improve beta-Cell Survival and Insulin Secretion in Three-Dimensional Culture. *Tissue Engineering Part A,* 14, 1959-1968.

Weber, L. M. , K. N. Hayda, K. Haskins & K. S. Anseth (2007) The effects of cell-matrix interactions on encapsulated beta-cell function within hydrogels functionalized with matrix-derived adhesive peptides. *Biomaterials,* 28, 3004-3011.

Weber, L. M. , C. G. Lopez & K. S. Anseth (2009) Effects of PEG hydrogel crosslinking density on protein diffusion and encapsulated islet survival and function. *Journal of Biomedical Materials Research Part A,* 90A, 720-729.

West, J. 2005. Bioactive hydrogels: Mimicking the extracellular matrix with synthetic materials. In *Scaffolding in Tissue Engineering* ed. J. Elisseeff, 275-281. Boca Raton, FL: CRC Press.

White, T. J. , W. B. Liechty & A. Guymon (2007) The influence of N-vinyl pyrrolidone on polymerization kinetics and thermo-mechanical properties of crosslinked acrylate polymers. *Journal of Polymer Science Part a-Polymer Chemistry,* 45, 4062-4073.

Woods, A. & J. Couchman (1998) Syndecans: synergistic activators of cell adhesion. *Trends Cell Biol,* 8, 189-191.

Woods, A. & J. Couchman (2000) Integrin modulation by lateral association. *J Biol Chem,* 275, 24233-24236.

Woods, A. , E. Oh & J. Couchman (1998) Syndecan proteoglycans and cell adhesion. *Matrix Biol,* 17, 477-483.

Yamaguchi, N. , L. Zhang, B. Chae, C. Palla, E. Furst & K. Kiick (2007) Growth factor mediated assembly of cell receptor-responsive hydrogels. *J Am Chem Soc,* 129, 3040-3041.

Zhang, J. , A. Skardal & G. Prestwich (2008) Engineered extracellular matrices with cleavable crosslinkers for cell expansion and easy cell recovery. *Biomaterials,* 29, 4521-4531.

Zhang, L. , E. Furst & K. Kiick (2006) Manipulation of hydrogel assembly and growth factor delivery via the use of peptide-polysaccharide interactions. *J Control Release* 114, 130-142.

Zhu, J. (2010) Bioactive modification of poly(ethylene glycol) hydrogels for tissue engineering. *Biomaterials,* 31, 4639-56.

Zhu, J. , J. Beamish, C. Tang, K. Kottke-Marchant & R. M. RE (2006) Extracellular matrix-like cell-adhesive hydrogels form RGD-containing poly(ethylene glycol) diacrylate. *Macromolecules* 39, 1305-1307.

Zhu, J. , C. Tang, K. Kottke-Marchant & R. Marchant (2009) Design and synthesis of biomimetic hydrogel scaffolds with controlled organization of cyclic RGD peptides. *Bioconjug Chem,* 20, 333-339.

Zhu, W., J. Latridis, V. Hlibczuk, A. Ratcliffe & V. Mow (1996) Determination of collageneproteoglycan interactions in vitro. *J Biomech* 29, 773-783.

Zisch, A. , M. Lutolf & J. Hubbell (2003) Biopolymeric delivery matrices for angiogenic growth factors. *Cardiovasc Pathol,* 12, 295-310.

Biomedical Engineering, Trends in Materials Science
Edited by Mr Anthony Laskovski

ISBN 978-953-307-513-6
Hard cover, 564 pages
Publisher InTech
Published online 08, January, 2011
Published in print edition January, 2011

Rapid technological developments in the last century have brought the field of biomedical engineering into a totally new realm. Breakthroughs in materials science, imaging, electronics and, more recently, the information age have improved our understanding of the human body. As a result, the field of biomedical engineering is thriving, with innovations that aim to improve the quality and reduce the cost of medical care. This book is the second in a series of three that will present recent trends in biomedical engineering, with a particular focus on materials science in biomedical engineering, including developments in alloys, nanomaterials and polymer technologies.

InTech Europe
University Campus STeP Ri
Slavka Krautzeka 83/A
51000 Rijeka, Croatia
Phone: +385 (51) 770 447
Fax: +385 (51) 686 166
www.intechopen.com

InTech China
Unit 405, Office Block, Hotel Equatorial Shanghai
No.65, Yan An Road (West), Shanghai, 200040, China
中国上海市延安西路65号上海国际贵都大饭店办公楼405单元
Phone: +86-21-62489820
Fax: +86-21-62489821

IntechOpen